

AD-A118 517

STANFORD UNIV CA CENTER FOR MATERIALS RESEARCH

F/S 18/4

LONG RANGE MATERIALS RESEARCH. SUPPLEMENT 2. EXCITONIC EMISSION--ETC(U)

JAN 77 O L HSU, C W BATES

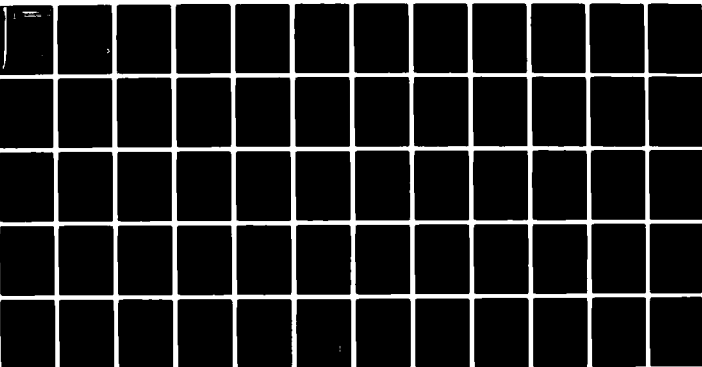
N00014-75-C-1171

UNCLASSIFIED

CMR-77-1-SUPPL-2

NL

1 x 1
4 sec



END
DATE
FILMED
9 82
DTIC

①

EXCITONIC EMISSION FROM CsI(Na)

by

Olive Lee Hsu
and
Clayton W. Bates, Jr.

Supplement 2 to Annual Technical Report CMR-77-1

Long Range Materials Research
Contract N00014-75-C-1171

Sponsored by
Defense Advanced Projects Agency

January 1977

DTIC
SELECTE D
S AUG 24 1982
A

This document has been approved
for public release and sale; its
distribution is unlimited.

EXCITONIC EMISSION FROM CsI(Na)

by

Olive Lee Hsu
Department of Materials Science and Engineering
Stanford University
Stanford, California 94305

and

Clayton W. Bates, Jr.
Department of Materials Science and Engineering
Stanford University
Stanford, California 94305



Suggestion For	
DTIC	<input checked="" type="checkbox"/>
AD	<input type="checkbox"/>
Unannounced	<input type="checkbox"/>
Classification	
Distribution/	
Availability Codes	
Avail and/or	
Dist	Special
A	

ABSTRACT

Photoluminescence in CsI(Na) was studied. This work used non-ionizing light sources and obtained the data from well-annealed, zone-refined specimens. A series of absorption excitation and emission spectra were measured at temperatures between 300°K and 4.2°K. There are strong absorption bands on the long wavelength side of the fundamental absorption edge of the host CsI crystal. The excitation spectra are closely related to the absorption bands. The emission spectra consist of the characteristic blue emission and other low temperature emissions. The emission spectra were decomposed into the superposition of Gaussian peaks by computer. It is found for the first time that the characteristic emission consists of two bands, centered at 4200 Å and 3700 Å respectively. The latter one increased as the temperature decreased.

The energies of localized excitons were calculated by employing a Born-Haber cycle. The calculated results were compared with the measured absorption and excitation spectra. Each absorption and excitation band was identified as the transition of either a free or a localized exciton. The most important one is the exciton created by transferring an electron from an iodine ion to a substitutional sodium ion. This localized exciton called "impurity" exciton is responsible for the absorption peak and the excitation band of the characteristic emission. The β exciton also contributes to this absorption and excitation at low temperatures.

A configuration coordinates diagram is proposed to explain the evolution of the two characteristic emission bands. The diagram consists of the ground state and two excited states.

Two polarization experiments were carried out in order to understand the symmetry of the characteristic luminescent center. Neither of the two characteristic emission bands was polarizable. The absorption spectrum of

an ultraviolet irradiated CsI(Na) crystal was measured at 15°K. No evidence of the existence of V_k centers was found. It is concluded that during the relaxation of "impurity" excitons, isolated V_k centers are not necessarily formed.

I. INTRODUCTION

Luminescence phenomenon in CsI(Na) is interesting both from a theoretical as well as a practical point of view. CsI(Na) is the best alkali halide X-ray detector now in use¹. It is also an excellent particle detector that has been used extensively in scintillation studies¹. Although, luminescence in the alkali halides has been studied quite intensively, most of the work has been done on systems with the sodium chloride structure. Information on the nature of luminescent centers in alkali halides with the cesium chloride structure and particularly those with nonisomorphic alkali metal impurities is still limited. This study of the CsI(Na) luminescence will partly fill this gap.

The majority of the previous studies²⁻⁹ in this area introduced ionizing radiations (X-rays, β rays, and etc.) and thus produced extra lattice defects in the specimens. Those^{7,10-13} which excited the specimens with non-ionizing ultraviolet light failed to obtain the details of the excitation spectra. There is lacking systematic work on the photoluminescence mechanism in CsI(Na). The conclusion concerning the nature of the luminescent center in CsI(Na) made in the previous works were based on the similarity of the luminescence from CsI(Na) and from CsI doped with divalent cation impurities and deformed CsI crystals. Direct corroboration of those conclusions have not been obtained and ambiguities and controversies still exist¹⁴. The temperature dependence of the major-emission band of CsI(Na) is opposite to that of CsI containing divalent cation impurities when excited with ionizing radiations or high energy particles. The work performed on deformed CsI crystals occurred during a period when the effects of trace quantities of sodium were not appreciated. Furthermore, there has not been reported any complete study of the whole emission spectra of CsI(Na) and the correlation among the different emission bands. There is also little published work on the structure of the major emission band of CsI(Na).

In order to resolve these difficulties, we performed a systematic measurement of the absorption, excitation and emission spectra of CsI(Na) at temperatures

between 300°K and 4.2°K. The absorption spectra cover the range 2.6 μ m to 190nm. The emission spectra are from 300nm to 800nm with excitations between 300nm and 190nm. The specimens used in the experiment were well-annealed, zone-refined CsI(Na) crystals. The sodium concentration in these crystals is 6ppm.

Calculations of the localized exciton energies were carried out by employing a Born-Haber cycle. The results were compared with the observed absorption and excitation peaks. The origins of these peaks were then elucidated.

The emission spectra were decomposed into the superposition of Gaussian peaks. The luminescent centers responsible for each emission band were identified by the corresponding excitation peaks. A configuration coordinate diagram was constructed to explain the evolution of the major emission bands of CsI(Na).

In order to understand the symmetry of the major luminescent center, two polarization experiments were performed. The results helped to postulate the relaxation process of the luminescent center.

Some of our preliminary results have been reported in previous publications¹⁴⁻¹⁷. Here we present the complete experimental results, the details of the data treatment and the conclusion drawn from them.

II. ABSORPTION SPECTRA AND LOCALIZED EXCITONS

A. Absorption Spectra of CsI(Na) Thin Films

The absorption spectra were measured by a Cary model 14R recording spectrophotometer. The absorption spectra of CsI(Na) were measured from bulk single crystals as well as from vacuum evaporated polycrystalline thin films. The procedures involved in preparing the thin films and the absorption spectra of these films were reported in reference 16. It was found there that the absorption spectra of the CsI(Na) thin films are the same as those of pure CsI¹⁹⁻²¹. At 300°K, there are two sharp exciton peaks located at 2225 \AA and 2085 \AA . At 77°K, the lower energy peak shifted to 2175 \AA while the higher energy one did not change

position but split into two peaks at 2095Å and 2080Å, respectively. The similarity between the absorption spectra of CsI(Na) thin films and pure CsI is due to the small amount of sodium ions along the optical path. This is the reason why the absorption spectra of CsI(Na) thin films were not pursued intensively in this work.

B. Absorption Spectra of CsI(Na) Bulk Crystal

The absorption spectra of CsI(Na) bulk crystal were taken at a series of temperatures from 300°K to 4.2°K with an interval of about 20°K. The specimens used were 2mm thick single crystals which had never been cooled to low temperatures nor had they been exposed to radiation except room light before the measurement. There are no appreciable absorption bands in the region from 2.6 μm to 350nm. From 350nm to 190nm, there are several absorption bands whose structure strongly depends on temperature. Part of the measured ultraviolet absorption spectra are given in Figures 1-6.

The most noticeable points in the absorption spectra are the appearance of the hump in the 2600Å-3200Å region and the strong, broad absorption step around 2400Å which shifts with temperature and defines the absorption edge of the CsI(Na) crystal. The hump on the low energy side of the absorption edge gradually builds up in strength to over 0.3 O.D. (optical density) as the temperature was lowered from 300°K to 4.2°K. The absorption edge shifted from 2450Å at 300°K to 2350Å at 4.2°K. At temperatures below 155°K, in the region just below the absorption edge, there was a broad shoulder with a not-clearly-defined structure. This low strength shoulder connected the absorption edge and the broad hump in the 2600Å-3200Å region

There are two peaks at 2250Å and 2175Å just below 300°K (Figure 2). The latter one gradually shifted to shorter wavelengths while the low energy one became a step. At 130°K, the peak shifted to 2130Å and reached its full strength while the step became a peak again at 2200Å. At the same time a shoulder around 2050-2000Å appeared. The last mentioned two peaks then decreased their height and could

not be resolved from each other. This peak continued to shift to shorter wavelengths while the absorption on the low energy side of this peak decreased as the temperature was lowered. Finally, at temperatures below 20°K, it met the edge below the 2050Å shoulder and became another shoulder.

From the above observation of the temperature dependence of excitonic absorption in CsI(Na) bulk crystals, we can identify the peaks at 2175Å at 285°K which changes location at lower temperatures with the lower energy peak in pure CsI¹⁹⁻²¹. However, the one at 2250Å at 285°K which changed structure and mixed together with the last named peak at lower temperatures needs a separate consideration. The higher energy peak in pure CsI which is a doublet at low temperatures appears in CsI(Na) as a shoulder around 2050-2000Å. The doublet cannot be resolved in this specimen.

The two absorption peaks which are observed both in pure CsI and CsI(Na) have been attributed to the transition of free excitons^{20,22,23}. The peak at 2225Å at RT which shifted to shorter wavelengths at lower temperatures was identified with $\Gamma_8^- \rightarrow \Gamma_6^+$ excitonic transition. The peak which splits into a doublet at lower temperatures was assigned to the exciton state formed from the $\Gamma_8^- \rightarrow \Gamma_8^+$ transition. The spin-orbit partners of these peaks are the $\Gamma_6^- \rightarrow \Gamma_6^+$ and $\Gamma_6^- \rightarrow \Gamma_8^+$ transitions at 6.9 eV which is out of the range of our measurement.

The absorption of CsI(Na) bulk crystal in the long wavelength side of the free excitonic absorption peaks includes:

- (1) a peak with energy slightly lower than the free exciton,
- (2) a broad, flat step around 2400Å-2300Å⁰ which defines the sharp absorption edge, and
- (3) a shoulder and a hump below the edge which extended into 3200Å.

All these absorption bands are not found in pure CsI. Because they have energies lower than the free excitons, they may be considered as the transition of excitons localized near the sodium impurities or other lattice defects whose existence is due to or enhanced by the sodium impurities.

In the following paragraphs, we carry out the calculation of energies of

excitons localized near the lattice defects which can possibly exist in CsI(Na) crystal.

C. Calculation of Localized Exciton Energies

The most commonly observed localized exciton absorptions in alkali halides are the α and β bands which are the transitions of the excitons created in the vicinities of a halogen ion vacancy and an F center, respectively. Bassani and Inchauspe²⁴ carried out a calculation on the position of the α and β bands relative to the first free exciton absorption in alkali halides with the sodium chloride structure. This method can be extended to calculate the energy of the excitons located at other defect configurations²⁵⁻²⁷. It can also be applied to calculate the localized exciton energies in alkali halides with the cesium chloride structure²⁸.

Figure 7 shows the configurations where an α exciton can be created in CsI. An electron on an iodine ion (called ion number 1) is transferred to a neighboring cesium ion (called ion number 2) in the presence of a nearby iodine ion vacancy (at the position called number 3). The four configurations differ from each other by different relative positions of ions 1 and 2 and the vacancy position 3. The (110) face of the CsI lattice is drawn because the nearest neighbor ions in the crystal are located on this face. To apply the result given by Bassani and Inchauspe²⁴ to the present system, we have to make proper adjustments to fit the crystal of CsI. The most important difference involved in the calculation between the sodium chloride and the cesium chloride structures is the number of nearest neighbors. In the sodium chloride structure, each ion has six nearest neighboring ions of opposite sign. In the cesium chloride structure, this number is eight. The repulsive energy between closed shells of electrons which is part of the potential energy at a lattice point is $\frac{\alpha_M e^2}{8r_0^2}$ in the cesium chloride structure and is $\frac{\alpha_M e^2}{6r_0^2}$ in the sodium chloride

structure.

The other important factors in the calculation are the lattice sums which are defined as:

$$S_+ = \sum_{\text{+ions}}'''' \frac{\cos(r_{2i}, r_{3i})}{r_{2i}^2 r_{3i}^2} - \sum_{\text{+ions}}'''' \frac{\cos(r_{1i}, r_{3i})}{r_{1i}^2 r_{3i}^2} \quad (1)$$

$$S_- = \sum_{\text{-ions}}'''' \frac{\cos(r_{2i}, r_{3i})}{r_{2i}^2 r_{3i}^2} - \sum_{\text{-ions}}'''' \frac{\cos(r_{1i}, r_{3i})}{r_{1i}^2 r_{3i}^2} \quad (2)$$

where r_{3i} is the distance between ion i and ion 3, etc. in the units of r_0 the cesium-iodine ion distance. The summations are over all positive or negative ion sites (as indicated) except that the sites 1, 2 and 3 are omitted as suggested by the triple prime. The values of S_+ and S_- are different in the two alkali-halide crystal structures. To obtain the results in the cesium chloride structure, a method similar to that developed by Rosenstock²⁶ for sodium chloride structure was employed. The numerical work was done on a HP9830 A calculator.

Employing the results given in reference 24 making the suitable adjustments, we obtained the positions of the α excitons at three temperatures. The results are listed in table 1.

Figure 8 shows the configurations where an exciton is created near a cesium ion vacancy. The calculation is similar to that of the α exciton energies²⁵. The results are listed in table 2.

Figure 7 can also be used to represent the configurations where a β exciton can be created if the iodine ion vacancies are replaced by the F centers, in other words if an electron is placed at each iodine vacancy. Again, we employed the formula similar to that given in reference 24 and obtained the position of the β bands in CsI at three temperatures. The results are listed in table 3.

Now, we consider an exciton created by transferring an electron from an iodine ion which has a sodium ion as one of its nearest neighbors to a cesium ion. The configurations for excitons of this sort can be referred to figure 8

if the cation vacancies are replaced by sodium ions. The only contribution to the energy difference between a free exciton and exciton in the vicinity of a sodium impurity is the difference of polarization energies of a cesium ion and a sodium ion. The results of $\Delta h\nu$ are: Case (I) - 0.036 eV, Case (II) - 0.027 eV, Case (III) - 0.029 eV and Case (IV) - 0.014 eV. The negative value of $\Delta h\nu$ means that the localized excitons have higher energies than the first free exciton. If the energy differences are converted into wavelengths, the differences are about 15\AA . This is within the experimental error. It is also worth mentioning here that the numerical values of ionic polarizability of cesium, iodine and sodium ions from several reference²⁹⁻³¹ are different. The variation in the final results of the calculated localized exciton wavelength when the values of ionic polarizability from different sources are used is about $\pm 20\text{\AA}$.

The sodium impurity may exist in the neighborhood of a lattice defect such as a vacancy and F center. Figure 9 shows some of the possible configurations for an exciton created near the defect complex involving a sodium impurity ion. The energy difference between the free exciton and a localized exciton of this sort is the sum of the difference of polarization energies of cesium and sodium ions and the quantities given in Tables 1-3 (with a slight modification of the lattice sums S_+ and S_-) according to the lattice defect involved in the complex. In other words, the effects on the localized exciton energy from each individual defect in the complex are additive. For example, the energy difference between the free exciton and the exciton (called β_A exciton) created near an F_A center (an F center with one of its nearest neighbors replaced by a sodium ion) can be expressed as:

$$h\nu_f - h\nu_{\beta_A} = (h\nu_f - h\nu_{\beta}) + (h\nu_f - h\nu_{Na}) \quad (3)$$

As indicated in the last paragraph the value of the second term in Eq. (3) is so small that it is impossible to distinguish a β_A exciton from a β exciton

in energy.

All the cases discussed above are for localized excitons created by transferring an electron from an iodine ion to a cesium ion in the vicinity of a sodium ion. The sodium impurity ion is not involved in the transition directly but only disturbs the energy states involved in the transition. However, sodium ions are very efficient electron traps,⁸ thus it is very likely that an exciton can be created by transferring an electron from an iodine ion to a sodium ion. We will call this kind of exciton an "impurity" exciton.

The binding energy for an electron trapped on a substitutional sodium ion in CsI has been calculated by Monnier³². The energy is given by the sum of the difference between the ionization energy of the sodium and the cesium atom and a correction for the fact that the electron at the bottom of the conduction band is delocalized. The result turned out to be 0.45 eV.

When sodium "impurity" exciton is created, the energy absorbed by the electron will be 0.45 eV less than that when a "host" exciton (i.e., an exciton created by transferring an electron from an iodine ion to a cesium ion) is created in the same configuration. Thus, the energy of a sodium "impurity" exciton in an otherwise perfect lattice is 0.45 eV less than the free exciton energy. The energy difference between a free exciton and a sodium "impurity" exciton localized at a defect-impurity complexity can then be expressed as:

$$h\nu_f - h\nu_{\text{sodium "impurity"}} = \Delta W + 0.45 \text{ eV} \quad (4)$$

where ΔW is the energy difference arising from the defect (vacancies, F center, etc.) involved. Figure 10 shows the configurations used to calculate the "impurity" exciton energy. The results are listed in Table 4.

Because ΔW in Eq. (4) is small compared with 0.45 eV except in cases (j) - (m) where an F center is involved in the defect complex, the wavelength of the impurity-exciton bands are almost indistinguishable from each other

according to the calculated results.

When the measured absorption spectra of CsI(Na) bulk crystals at different temperatures are compared with the calculated results of the localized exciton energy, the following conclusions may be drawn.

First, the peak at 2310 Å at 4.2°K which shifted to 2330 Å at 70°K and showed as a shoulder around 2400 Å at RT agrees best with the calculated values of the β band exciton of case (I) in Figure 7 and with that of a sodium "impurity"-exciton in an otherwise perfect lattice [case (a) in Figure 10]. Because the calculated energies of the last named localized excitons are almost identical, it is impossible to favor either of them from the energy aspect. However, in view of the fact that this band is absent in pure CsI absorption and the crystal whose absorption spectra are reported here had never been subjected to any strain or irradiation before the measurement was made, it is not likely that the concentration of F centers at RT was high enough to produce a strong β band. Furthermore, electrical conductivity measurements³³ shows that small amounts of sodium in CsI does not affect the conductivity which is due mainly to the moving of anion vacancies. Thus, sodium ions in CsI do not increase the concentrations of anion vacancies and F centers. This measured absorption band is then more likely to arise from the "impurity"-exciton transition at temperatures not too far below 300°K. At lower temperatures, F centers may be created due to the thermal expansion coefficient mismatch between the specimen, the vacuum grease, and the copper block which constitute the sample holder in the experimental dewar. This phenomenon was observed in pure CsI crystals³⁴. Thus, β exciton absorption may be superimposed on the impurity-exciton absorption at lower temperatures. In fact, the flatness on the high energy side of this peak may indicate that this absorption band is the superposition of several bands, including the impurity band [case (a)] and different β bands.

Second, the low intensity shoulder in the region between 2600 Å and the absorption edge is best described by the impurity exciton at an F_A center [case (j) - (m) in Figure 10]. Its appearance at low temperatures supports the hypothesis that the F center was created at low temperatures.

Third, the absorption band at 2200 Å at 130°K which shifted position and mixed with the first free exciton at lower temperature may be attributed to the α excitons. This band started to show up at the same temperature (about 130°K) as the absorption of the impurity exciton at an F_A center became appreciable. This is an indication that the concentrations of iodine vacancies and F centers which are created due to cooling are high enough such that the β band absorption also sets in at this temperature.

The energies of the excitons near a cesium ion vacancy are close to those of α excitons. It is improper to exclude the possible contribution from excitons of this sort. However, because iodine ions are more mobile than cesium ions in the crystal, it is easier to produce an iodine ion vacancy than a cesium ion vacancy. Thus, the contribution of α excitons to this absorption band is probably higher than that of an exciton near a cesium ion vacancy.

The absorption hump in the region from 3200 Å to 2600 Å does not match any of the calculated results. Because it is located at the long wavelength side of the absorption band due to excitons localized at simple defects (vacancies, F centers, etc.), it is easy to imagine that this absorption may arise from the excitonic transitions in the vicinity of complicated defect clusters or the specimen surface. This point of view is supported by the fact that this hump is higher in the absorption spectra of a crystal which has been temperature cycled several times and subjected to UV radiation before the absorption measurement. The defect density in this crystal is high and the surface is damaged. The flatness of the hump indicates that it is not a single band absorption and that the lattice distortion around the defects

which is neglected in the calculation is not negligible in this case.

We should mention at this point that according to Bassani and Inchauspe²⁴ the energy of α excitons should be lower than that of β excitons. However, the results presented here are just the opposite. No satisfactory explanation can be made except that the intuitive statement by Bassani and Inchauspe does not hold for crystals with the cesium chloride structure.

Summarizing from the above, the absorption spectra of CsI(Na) bulk crystals can be explained by excitonic transitions. The energies of localized excitons can be calculated from a Born-Haber cycle. The calculated results indicate that the excitons which are responsible for the absorption are (from high energy to low energy excitons) α excitons, β excitons and impurity excitons in an otherwise perfect lattice (the latter two have the same energy), impurity excitons at F_A centers, and excitons near complicated defect clusters and crystal surfaces.

D. Absorption Measurement Concerning V_k Centers

It has been found that V_k centers can be formed in CsI(Na) after x-ray irradiation at low temperature^{8,35}. Sidler, et al.⁸ irradiated CsI(Na) crystals which contained 200-300 ppm of sodium with x-rays at liquid helium temperature for 1 minute and found an absorption band at 4100 Å. This band was polarizable along the [100] direction and thus was recognized as due to V_k center absorption. From thermoluminescence studies, Sidler, et al. also found that V_k centers move by linear migration above 60°K and by 90° jumps above 90°K.

Since x-ray and ultraviolet light stimulate the same blue emission from CsI(Na), it is interesting to see whether ultraviolet light also produces V_k centers in this materials at low temperatures. For this purpose we carried out an experiment which consisted of taking the absorption spectra of a CsI(Na) crystal before and after UV irradiation at 15°K. The absorption spectra of a 2 mm thick CsI(Na) crystal was measured at 15°K with the Cary-14R

spectrophotometer equipped with a slide wire which records 0-0.1 O.D. on a ten-inch wide chart paper. This is ten times more sensitive than the slide wire used in measuring the UV absorption spectra reported in Figs. 1 through 5. This crystal was then irradiated for 3½ hours at 15°K with UV light (2000-2200 Å) from a high pressure mercury lamp connected with a monochromator. The absorption spectrum was then measured again at the same temperature. The optical density of the absorption spectrum before UV irradiation was then subtracted from that of the spectrum after irradiation. The result is shown in Figure 11. Three bands are found in this spectrum. There is a narrow band of magnitude 0.028 O.D. (i.e., 0.32cm^{-1}) peaking at 4300 Å which is 200 Å away from the V_k band measured by Sidler, et al.⁸

Because the absorption coefficient is low at the measured peak and the original spectra are noisy due to the high sensitivity of the spectrophotometer, it is improper at this point to make any positive conclusion about this experiment. But the result is encouraging and further study is suggested by these preliminary results.

III. EMISSION AND EXCITATION SPECTRUM OF CsI(Na)

A. Experimental Procedures

To measure the emission and the excitation spectra of CsI(Na), a conventional arrangement as shown in Figure 12 was used. The light source was a Bausch and Lomb deuterium lamp which had a fairly smooth spectrum from 2000 Å to 4000 Å without any sharp lines. The light went through a grating monochromator which was equipped with a scanning motor and then through a mechanical chopper. The chopped monochromatic light was incident upon the large face (1.3 cm x 1.3 cm) of the sample in the dewar. The emission from the sample was measured at right angles to the exciting light in order to avoid interference between the transmitted and reflected light. Passing through another monochromator, the emission was detected by an RCA 8645 photomultiplier

tube with an S-20 spectral response. The output of the tube was fed into a lock-in amplifier which was tuned to the frequency of the chopper and then recorded by a strip chart recorder.

The excitation spectrums cover the range from 2000 Å to 3000 Å. Some were extended to 3500 Å. The emission spectrums are measured from 3000 Å to 5000 Å. The wavelength readings of the monochromators were calibrated with the spectral lines of a high pressure mercury lamp. The emission spectrums were corrected for the spectral response of the photomultiplier tube. However, most of the emission spectrums match the S-20 spectral response so well that the correction is negligible except at wavelengths around 3000 Å.

The corrected emission spectrums were analyzed by a least-squares fitting program on a PDP-10 computer. The numbers, the positions, the heights and the widths of Gaussian peaks whose superpositions fit the emission spectrums best were determined. The decomposition of the excitation spectrums into Gaussian peaks is difficult to accomplish by computer. Because the excitation spectra are narrow, the number of input data points is small. However, there are three parameters in the program for each Gaussian peak, i.e., the height, the width and the position of the peak. The degree of freedom of the program which is the revised number of data points minus the number of parameters is very small. The computer program was then unable to get a reasonable result. The decomposition of the excitation spectrums was done by observation. A series of excitation spectrums of adjacent emission wavelengths were taken. The evolution of the excitation bands was revealed by comparing these excitation spectrums.

B. The Characteristic Emission and Excitation Spectrums of CsI(Na) Crystals

The major emission from bulk crystals of CsI(Na) when excited with

ultraviolet light or ionizing radiations is blue light with λ_{max} around 4200 Å^{11,12}. In a preliminary experiment¹⁶ we found that this blue emission was absent in thin films of CsI(Na) about 200 Å thick and was very weak compared with the intrinsic emission of pure CsI at liquid nitrogen temperature in thin films about 6000 Å thick. It was also found that the emission and excitation spectrums were modified by the heat treatment the specimens received before the optical measurement. In order to avoid the influence of the heat treatment and to elucidate the effect of the sodium impurity on the luminescence properties of CsI(Na), it is necessary to perform the measurement on CsI(Na) bulk crystals which have never been irradiated before the measurement and whose defect concentration (other than the desired impurity content) is low.

Figures 13-16 are the major emission and the corresponding excitation spectrums taken from CsI(Na) crystals of this sort at several temperatures. The dash-dot curves in the emission spectrums are the Gaussian peaks fitted by the computer analysis. That in the excitation spectrums were fitted by observation. The most striking point of the measured emission spectrums is that they actually consist of two bands, one peaking around 4200 Å and the other one around 3700 Å. This feature has not been reported before.

The peak position of these two emission bands varied within a 100 Å range. It is difficult to tell whether this variation is due to the nature of these emission bands or is due to the interference with other emission bands and the uncertainty of the computer analysis. The halfwidth of the 4200 Å band is 0.64 eV at 300°K and gradually decreased to 0.33 eV at 4.2°K. The halfwidth of the 3700 Å band lies within the range from 0.33 eV to 0.24 eV at different temperatures. However, because the error of the computer result in peak halfwidth is about 0.15 eV this variation is within the error range. It is difficult to establish a well-defined relation between the temperature and the halfwidth of the 3700 Å emission band.

The intensity of the high energy peak relative to that of the low energy one increased about 4.5 times as the temperature decreased from 300°K to 4.2°K. The relative intensity also depended on the excitation energy. This point will be discussed later. The data showed that the emission intensity did not change much with temperature when the crystal was excited at the peak of the corresponding excitation spectrum. The intensity had small variations at different temperatures which may be due to the slightly different alignments of the instruments between measurements.

The excitation spectrums of this characteristic emission shifted toward higher energies as the temperature decreased. At 300°K the excitation spectrum is a single peak centered at 2450 Å. There is no difference between the excitation spectrums of the 4200 Å and 3700 Å emission band. This possibly results from the low intensity of the 3700 Å band at this temperature. In fact, the contribution to the intensity at 3700 Å from 4200 Å band is even higher than that from the 3700 Å band. It is impossible to separate these two emission bands from each other in measuring the excitation spectrum. Thus, when we set the monochromator on the emission side at 3700 Å and measured the corresponding excitation spectrum at room temperature, we were essentially measuring the excitation spectrum of the 4200 Å band. As the temperature decreased, the excitation spectrum deviated from a single Gaussian peak. At 130°K the excitation spectrum peaked at 2400 Å. However, it can be decomposed into the superposition of three Gaussian peaks centered at 2400 Å, 2325 Å and 2250 Å respectively. When the crystal was excited at the two higher energy bands, in addition to the characteristic emission, other emission bands were also observed which will be discussed in the next section. The intensity of several weak excitation bands with wavelengths longer than 2500 Å increased as the temperature decreased. The peak position of the three Gaussian bands shifted gradually to 2320 Å, 2250 Å and 2170 Å at 4.2°K for the 4200 Å emission. The lowest energy

peak is located at slightly longer wavelengths (about 15 Å) for the 3700 Å emission. The difference between the relative intensities of these two emission bands at 4.2°K when the crystal was excited at 2320 Å and 2370 Å clarifies part of this feature [Fig. 16(a)]. The intensities of the two higher energy excitation bands relative to the major (i.e., the lowest energy) peak of the 3700 Å emission were lower than that of the 4200 Å emission. From Figs. 16(b) and (c) we can also see the different structure at the long wavelength tail of the excitation spectrums of these two emission bands.

At this point we will turn our attention to other emission bands which were observed at low temperatures and try to identify their origins. This will hopefully clear up some of the controversial points about the luminescent nature of CsI(Na).

C. Other Emission Bands and Their Origins

In addition to the characteristic blue emission, we measured several other emissions from CsI(Na) at low temperatures. These emissions were weak compared with the major one and generally speaking, their intensities increased as temperature decreased. The corresponding excitation spectrums were closely related to the excitonic absorption spectrums. We will try to identify the origins of these emissions by comparing the excitation and the excitonic bands absorption.

It has been observed³⁶ that at temperatures between 20°K and 140°K, pure CsI has an emission peaking at 3380 Å when the crystal is excited in the free exciton bands. At liquid helium temperatures, this excitation also yields an emission band centered at 2900 Å whose intensity decreases rapidly with increasing temperature and is unmeasurable above 25°K. In our experiment, we observed an emission band around 3450 Å when the crystal was excited in the free exciton region. However, this emission was not isolated from other emissions, such as the characteristic emission of CsI(Na). This is understandable because the blue emission can also be excited in the free excitonic bands as shown by the excitation spectrums in Figs. 13-16. Figure 17 gives the emission

spectrums at several temperatures when the crystal was excited in this region.

Figure 18 is the corresponding excitation spectrums. The highest excitation peak is the one due to the characteristic emission because this blue emission extended into the 3450 Å region. The arrow in the figure indicates the peak of our interest at this point.

We did not observe the 2900 Å emission as reported in Ref. 36. At temperatures below 25°K, there are several excitation bands [Figs. 16, 18, 20, and 22(b)] for all emissions and also absorption bands around 2600 Å - 2900 Å. Furthermore, the photomultiplier tube used in the experiment has very low sensitivity in this region. Thus, it is very possible that this emission was re-absorbed by the crystal and excited other emissions and could not be detected.

However, there was another emission band peaking around 3100 Å which appeared at temperatures below 130°K. Figure 19 shows this emission spectrum at several temperatures. The excitation peak for this emission was located at a lower energy than that for the 3450 Å. This can be seen by comparing the excitation energies in Figs. 18 and 19. Figures 20(a) and (b) are the excitation spectrums of the 3100 Å and 3450 Å emissions at two temperatures. Again the peaks of our interest at this point are indicated by arrows. At 4.2°K, the excitation peak at about 2200 Å was greatly reduced while the low energy bands increased drastically. Figure 20(c) shows the excitation spectrums of emission at 3100 Å and 3400 Å at 4.2°K.

The 3450 Å emission has been attributed to the radiative recombination of relaxed free excitons. The 3100 Å emission whose excitation energy is right below that of the 3450 Å emission can then be assigned to the recombination of relaxed "host" α excitons because the "host" α exciton has its energy right below the first free exciton as shown in Section II. We have to mention here that the wavelength readings of the absorption and excitation peaks do not agree with each other exactly. This is possibly due to the calibration of the two spectrometers used. However, the relative position of these peaks makes the above assignment reasonable. This assignment is further confirmed by the same

temperature dependence of the α band absorption and the 3100 Å emission, i.e., both of them started to show up at 130°K and disappeared below 20°K. The disappearance of the α exciton absorption and excitation can be explained in the following way: At temperatures below 20°K the defect density was so high that defect clusters or complexes were formed. Thus the α band decreased rapidly while the long wavelength tail of the absorption and excitation spectrums which is due to the excitons localized near the defect cluster or specimen surface increased drastically.

When the CsI(Na) crystal was excited in the long wavelength region mentioned above at 4.2°K, the strongest emission band was located at 4500 Å, together with other weaker bands. This emission was observed at temperatures below 100°K; however, the intensity was not strong enough to give a well-defined spectrum until 20°K. Figures 21 and 22 are the emission and excitation spectrums of this emission at 20°K and 4.2°K. For comparison, those of the characteristic emission are also shown in these figures. Figure 22 shows that the major excitation peak of the long wavelength side of the 4500 Å emission was located at a slightly lower energy than that of the 4200 Å emission. Figure 21 clearly shows that the 4500 Å is a new low temperature emission and should be distinguished from the characteristic emission. Furthermore, the major excitation peak at 2400 Å is not the residue from the characteristic emission as in the case of the 3450 Å emission, while the one at 2200 Å is the residue because the emission spectrum of CsI(Na) with this excitation did not show any trace of the 4500 Å emission band (Fig. 23). In view of the excitation energy and the temperature dependence, the 4500 Å emission can be well described as the radiative recombination of relaxed excitons localized near the defect cluster and the "impurity" α and β excitons. The latter two dominated at temperatures above 4.2°K.

The long wavelength tail appeared in the excitation spectrum of all the emission bands at low temperatures. Since these excitation bands are in the

same region of the absorption as that due to excitons localized near defect clusters as proposed in Section II, the configuration around the luminescent centers created by this excitation should be complicated. We hypothesize that after the excitation the lattice around the center could relax into any of the configurations which were the same as those around the centers created by higher energy excitation. The excitons then recombined and gave the same emission as those excited by the higher energy bands. The complexity of the emission spectrums under this low energy excitation reveals the complexity of the corresponding luminescent centers.

Summarizing the above, there were low temperature emission bands from CsI(Na) crystals. The one centered at 3450 \AA has been investigated by other authors and was ascribed to the radiative recombination of free excitons. Besides this free exciton emission, we observed emissions centered at 3100 \AA and 4500 \AA . Based on the temperature dependence and the excitation energy, the former one was assigned to the radiative recombination of relaxed "host" α excitons while the latter one as that of relaxed "impurity" α and β excitons. The relaxed excitons near the defect clusters which can be excited by $2600 \text{ \AA} - 2900 \text{ \AA}$ light gave a complicated emission spectrums composed of all the observed emission bands in CsI(Na).

D. Emission Polarization Experiment

In order to understand the structural symmetry of the luminescent centers in CsI(Na) and thus help to make conclusions concerning the luminescence mechanism in CsI(Na) two emission polarization experiments were carried out.

The first polarization experiment was designed to find out the relation between the polarization of the excitation and emission light. The arrangement of the experiment is shown schematically in Figure 24. The sample used in this experiment was a single crystal of cesium iodide doped with 6 ppm

sodium which was cut and polished along (100) faces. The exciting light fell on the (010) face and the emitted light was observed at right angles to the (001) face. Ultraviolet-visible linear polarizers from Ealing were used to polarize the exciting light and to analyze the emission. A filter was used to separate the 4200 Å and 3750 Å emission. The reason for using a filter instead of using a monochromator is that the monochromator is able to produce a polarization as much as 0.3 [Polarization = $(I_{\parallel} - I_{\perp}) / (I_{\parallel} + I_{\perp}) = 0.3$]. This effect could account for the polarization artifact reported by Edgerton³⁷ who measured the polarization of the emission from KI(Tl) with a similar arrangement but used a grating monochromator in the emission side. The neutral density filter in front of the photomultiplier tube was used to cut down the light input into the tube and thus to avoid saturating the tube.

The excitation light was polarized with the electric field along [100], [001] and [101] directions. In each case, the polarization of the emission light was measured by rotating the polarizer (2) and the emission intensity was recorded for every 10°. The crystal was held at 4.2°K during the measurement. Neither the 4200 Å nor the 3750 Å emission band showed any polarization. Although there was a small variation (about 5%) of the emission intensity as the polarizer (2) rotated, this variation was independent of the excitation polarization and thus was believed due to the slight misalignment of the optical components. The polarization of the whole characteristic emission (i.e., without the filter) was also measured and the same result was obtained. We then conclude from this experiment that the characteristic emission of CsI(Na) is non-polarizable.

The second polarization experiment was designed to find out whether the V_k center is directly associated with the characteristic luminescence of CsI(Na). It has been found that in CsI(Na) crystals having aligned V_k centers in a [100] direction, the intrinsic recombination luminescence at 290 m, and 340 nm produced by optical excitation of the traps exhibits a partial plane polarization having essentially a σ character with respect to the axis of the parent V_k center

$(P = (I_{\parallel} - I_{\perp}) / (I_{\parallel} + I_{\perp})) = 0.2$. Thermoluminescence of CsI(Na) crystals X or β irradiated at 4.2°K showed that the characteristic emission is the radiative recombination of V_k centers with the trapped electrons⁸. It is then of interest to see whether V_k centers are produced in CsI(Na) crystals under ultraviolet irradiation and then involved in the characteristic luminescence process via the emission polarization measurement. Figure 25 is the experimental arrangement for this experiment. The single crystal of CsI(Na) which was cut and polished along the (100) faces was kept at 20°K which is below the V_k center migration temperature⁸. The crystal was illuminated simultaneously with chopped ultraviolet light at 2350 Å where the peak excitation of the characteristic emission is located at 20°K and constant intensity blue light at 4100 Å where the V_k absorption band is located. The blue light was polarized along the [100] direction. The blue and ultraviolet lights were incident upon the two large (010) faces of the specimen from opposite directions. The emission light was measured at right angles to the exciting and aligning lights from the (001) face. As would be expected, scattered 4100 Å blue light caused a signal to appear in the output of the lock-in amplifier even when the crystal was not luminescing. To correct for this, the scattered light was measured with the ultraviolet light off. The result showed that the scattered light was very weak, only about 1% of the luminescence intensity. The background of scattered light determined in this way was subtracted from the readings taken with the ultraviolet light on.

Presumably if V_k centers were produced under the 2350 Å excitation, they would then be aligned by the polarized 4100 Å light along [010] and [001] axes. The electrons recombining with the aligned V_k center would yield an emission polarized in the same directions. In other words, if the V_k centers were produced by the 2350 Å irradiation and were involved in the luminescence process, with the arrangement shown in Fig. 25, we would have measured the characteristic emission light polarized along the [010] direction. The result we obtained was negative. Neither of the two major emission bands was polarized.

Assuming that the 2350 Å light is in the localized exciton region and does not have enough energy to produce stable hole and electron centers, we then tried producing V_k centers by ultraviolet light in the free exciton region. The crystal was illuminated simultaneously with chopped 2100 Å ultraviolet light and polarized 4100 Å blue light of constant intensity at 20°K for ten hours. The monochromator (1) was then shifted to 2350 Å while the monochromator (2) was still maintained at 4100 Å. The emission polarization was measured and again the result was negative. No polarization of the characteristic emission was found.

The result of the first polarization experiment shows that there is no correlation of polarization between the characteristic exciting and emitted radiations. This result suggests that the exciton created by the characteristic exciting band loses the memory of polarization if there is any during the relaxation process. The result of the second experiment suggests that isolated V_k centers and trapped electrons are not formed in CsI(Na) under ultraviolet light. These results are consistent with the result of absorption measurement in Section II.

E. Photoluminescence Mechanism in CsI(Na)

We shall now attempt to identify the luminescent center in CsI(Na) crystals which is responsible for the characteristic blue emission. The peak excitation energy of this emission agrees very well with the "impurity" exciton energy. It is natural to ascribe this emission to the radiative recombination of a relaxed "impurity" exciton. However, on the other hand, the calculated energy of the "host" β exciton has energy only slightly higher than that of the "impurity" exciton. Moreover, the excitation spectrum of this emission consists of three closely spaced Gaussian peaks. It¹³ has been found that the CsI crystals containing the divalent impurity cations Cs^{2+} , Sr^{2+} , Ba^{2+} and Mn^{2+} and deformed pure CsI crystals have luminescence properties similar to that of CsI(Na). It is obvious that a sodium "impurity" exciton cannot be the origin of the luminescence in the divalent impurity doped crystals. The assignment of the characteristic

emission as due to sodium "impurity" excitons then needs further consideration.

To solve this difficulty, it is worthwhile to consider the effect of the heat treatment the specimen received before the emission measurement. It has been mentioned at the beginning of this section that the heat treatment modified the excitation spectrums of the blue emission of CsI(Na). Figure ²⁶ shows the excitation spectrum of two specimens at liquid nitrogen temperature. Type I crystal is the crystal which did not receive any heat treatment before the emission measurement. Type II crystal had been heated to 500°C, kept at that temperature for one hour, and cooled to room temperature within four hours before the measurement. It is expected that type II crystals have much higher vacancy concentrations than type I crystals. The excitation spectrum of the type I crystal has a peak at 2380 Å and a shoulder at 2300 Å. For the type II crystal, the excitation spectrum is a single peak at 2315 Å which is evidently the same band as the 2300 Å shoulder in the excitation spectrum of the type I crystal. This result shows that the CsI(Na) crystal which has a higher vacancy concentration has a excitation spectrum different from that of a crystal with a low vacancy concentration.

Another fact that will help is that the excitation spectrum of the blue emission from a mechanically deformed pure CsI crystal or CsI crystal with 1 ppm sodium impurity (which is lower than that for optimum luminescence efficiency, i.e., 6 ppm) has the same character as that found in the excitation spectrum of the type II crystal (heat-treated) crystal. The excitation peak of the deformed pure CsI crystal is located at a wavelength about 100 Å shorter than that of the undeformed crystal with 6 ppm sodium content¹⁵. The crystal with 1 ppm sodium content which had a weak emission at 420 nm - 430 nm before deformation exhibited a very intense emission centered at 425 nm after deformation while the excitation peak shifted 100 Å toward shorter wavelength¹⁵.

The characteristic emission of CsI(Na) consists of two bands centered at 3700 Å and 4200 Å respectively. The former one increases as temperature

decreases. The existence of this emission band is not observed in the strained or divalent cation doped CsI crystals. Furthermore, the excitation spectrums of the two bands are not completely the same. The relative height of the 2280 Å band to the 2320 Å band at 4.2°K for the 3700 Å emission is lower than that for the 4200 Å [Figs. 16(b) and (c)]. When the crystal was excited at 2280 Å at 4.2°K the intensity of the 3700 Å band was low. Figure 26 clarifies this fact.

We now recall that the calculated results in Section II showed that the energies of the "host" β excitons created in four different lattice configurations are slightly higher than that of the "impurity" exciton. It is then clear that the major excitation peak of the CsI(Na) crystal with 6 ppm sodium content is due to the "impurity" exciton while the one at slightly shorter wavelength which is the major peak in heat-treated or mechanical-deformed crystal is due to "host" β excitons.

The characteristic excitation spectrum of the zone-refined CsI(Na) crystal at room temperature is a single Gaussian peak which according to the discussion above is due to an "impurity" exciton. At lower temperatures, both of the bands due to "impurity" excitons and "host" β excitons exist in the excitation spectrums. As discussed in Section II, F centers can be created in CsI crystals by cooling. The appearance of the β excitation band at temperatures below 175°K is consistent with the absorption measurement. The low intensity of the β excitation band for the 3700 Å emission and the fact that the 3700 Å emission is missing from the deformed and divalent cation doped CsI crystals are also consistent with each other.

The ambiguity about the assignment of the characteristic blue emission to the radiative recombination of sodium "impurity" exciton is then removed. Although the blue emission of the heat-treated or mechanically deformed CsI crystals has the same peak position as that of the CsI(Na) crystal, the composition of the emission spectrums and of the corresponding excitation

spectrums are different in details. The blue emission in the strained CsI crystal is then ascribed as due to the recombination of "host" β excitons. This "host" β excitation also contributes part of the 4200 Å band from CsI(Na) crystal at low temperatures but not the 3700 Å band.

The emission polarization and V_k center absorption experiments show that isolated electron and hole centers are not necessarily formed by ultra-violet light. The recombination of relaxed "impurity" excitons is direct. Charge transfer and defect diffusion are then not involved in the luminescence process. Lack of or small temperature dependence of the peak emission intensity also suggests this.

The configuration diagram shown in Figure 27 explains schematically the evolution of the two observed components of the characteristic emission. Excitation in the sodium "impurity" excitonic absorption band is followed by a relaxation to the first relaxed state (I) of the localized exciton, which exhibits the emission at 3700 Å. The second relaxed excitonic state (II) is reached over an energy barrier E_1 . The emission from this level gives the 4200 Å emission component. The value of E_1 can be determined by the temperature dependence of the quantum efficiency of the 3700 Å emission band which was not measured in our experiment. However, because the 4200 Å emission band is not quenched even at 4.2°K, the value of E_1 should be very small. E_1 is estimated to be in the order of 10^{-4} eV. There is the possibility that the relaxation of the second excitonic state (II) will lead to a non-radiative transition to the ground state at high temperature. This high temperature quenching phenomenon has not been observed in the temperature range from 4.2°K to 300°K in our experiment. It is then expected that the energy barrier E_2 for the nonradiative transition should be high at least in the order of 10^{-1} to 1 eV if it exists. The dotted part of the ground and the second excitonic state in the configuration diagram indicates that the structure there is still questionable.

The lifetime of the characteristic emission of CsI(Na) crystals has been measured by Naumenko and Panova³⁸, and Bates³⁹. For an increase in the temperature from 80°K to 300°K, the lifetime decreases exponentially from 4 μ sec to 0.4 μ sec. This temperature dependence of lifetime can be explained by the double-band feature of the emission. Each of the excited states is characterized by a decay time. At room temperature the majority of the emission comes from the transition from the second excited state (II) to the ground state. The lifetime of the emission at 300°K is determined by the decay time of the second excited state (II). At low temperatures the emission consists equally of the transition from the two excited states to the ground state, the lifetime of the emission then depends on the decay time of both excited states. Reference⁴⁰ gives a complete treatment of a similar problem on the intrinsic emission of CsI.

In summary, the characteristic emission of CsI(Na) crystals can be ascribed to the radiative recombination of relaxed sodium "impurity" excitons. A careful comparison of the emission and excitation spectrums of untreated CsI(Na) and heat-treated or mechanical-deformed CsI(Na) shows that although the luminescent properties of these two kinds of specimens resemble each other closely, they are actually different. The emission of the strained CsI crystal is assigned to the recombination of relaxed "host" β excitons. This "host" β excitonic emission also contributes part of the 4200 Å band in the CsI(Na) emission at low temperatures. A proposed configuration diagram can be used to explain the evolution of the two components and the temperature dependence of the lifetime of the characteristic emission. The details of this configuration diagram need more investigation which will be discussed in the next section.

IV. CONCLUSION AND DISCUSSION

It has been pointed out at the beginning of this paper that in spite of the importance in theoretical studies and practical applications, luminescence

phenomena in CsI(Na) have not received a thorough investigation. The conclusion of the luminescence center in CsI(Na) made in previous works were based on the similarity of the luminescence from CsI(Na) and the CsI doped with divalent cation impurities or deformed. Doubts about these conclusions still exist.

We approached this problem from a different direction. A systematic optical absorption and photoluminescence measurement was carried out on well-annealed and zone-refined CsI(Na) crystals at temperatures between 300°K and 4.2°K. The measured absorption, excitation and emission spectra were carefully examined and the evolution of each band in these spectra were revealed. The energies of the absorption and excitation peaks were compared with the energies of localized excitons calculated from a Born-Haber cycle. The luminescence centers in CsI(Na) were then identified.

This approach whose conclusions are directly based on the excitonic energies appears to work quite well. Each peak in the absorption spectrum can be identified as either a free exciton or an exciton localized near a certain lattice defect. Among all the localized excitons (Figs. 7-10), the most important one is the sodium "impurity" exciton which is the exciton created by transferring an electron from an iodine ion to a sodium ion which substitutes one of the nearest neighbors of the iodine ion in an otherwise perfect CsI lattice. The "impurity" exciton is responsible for the strong absorption step around 2400 Å at 300 Å which gradually shifted to 2320 Å at 4.2°K (Figs. 1-6). The calculated energies of the "host" β excitons which are the excitons created by transferring an electron from an iodine ion in the vicinity of an F center are slightly less than that of the sodium "impurity" excitons. The superposition of the "host" β excitons and "impurity" exciton explains the broadness and flatness of the high energy side of this absorption step at low temperatures.

Other measured absorption bands may be ascribed as the transition of excitons localized near an iodine ion vacancy, an F_A center, and defect clusters

respectively. These absorption bands increase in intensity as the temperature decreases.

The CsI(Na) crystal exhibits a strong blue emission under ultraviolet excitation. In our measurement, it is the first time that this characteristic emission is found to consist of two components, centered at 4200 Å and 3700 Å respectively. The latter one increases as temperature decreases. The excitation spectrums lead us to the conclusion that the characteristic emission is the radiative recombination of relaxed sodium "impurity" excitons. The evolution of the two components in this emission can be explained by a configuration coordinates diagram (Fig. 28).

It is also concluded from the excitation spectrums that the blue emission from a strained pure CsI crystal is due to the recombination of relaxed "host" β excitons. At low temperatures, this "host" β emission also contributes to the 4200 Å band in the CsI(Na) crystal emission, but not to the 3700 Å band.

The other emission bands which occur at low temperature can be attributed to the recombination of the excitons localized at different lattice defects. Again, these conclusions are based on the excitation energies of the emissions.

The importance of excitation spectrums in understanding the luminescence phenomenon is clearly demonstrated by this work. It is regrettable that in many luminescence studies, details of excitation spectrums were not available.

The configuration coordinates diagram (Fig. 28) proposed in this work is not complete. The interaction between the second excited state (II) with the ground state needs more investigation. To elucidate this interaction, the emission and excitation measurement should be extended to temperatures higher than 300°K. However, caution must be taken as the CsI crystal will undergo a structure transformation at high temperatures.

The temperature dependence of the lifetime and of the quantum efficiency of the two characteristic emission bands is necessary to determine the decay time of the two excited states and the value of the two potential barriers

E_1 and E_2 . However, we will expect difficulties in separating the "impurity" excitonic emission and the "host" β excitonic emission at 4200 Å. Extremely narrow bandpasses will be necessary for the excitation monochromator in order to separate these two excitation bands. It will also be helpful to carry out the F band absorption so that the concentration of F centers and thus effect of the "host" β excitonic emission can be determined.

The polarization experiments we carried out show that neither of the two characteristic emission bands is polarizable. This result is somewhat unexpected. It is an accepted theory⁴⁶ that excitons in alkali halide crystals become self-trapped during relaxation. The hole component is located in two neighboring halide ions and forms a quasimolecular V_k center. Electrons recombining radiatively with the V_k centers will give an emission with the electric field parallel or perpendicular to the axis of the V_k center. The excitonic emission from an alkali halide crystal populated with aligned V_k centers will be polarized. The results of our experiments show that either the V_k state was not reached before the electron-hole recombination occurs or the orientation is lost during the relaxation process. Moreover, the result we obtained from the absorption of an ultraviolet irradiated CsI(Na) crystal shows that V_k centers do not exist in the crystal or if they exist the concentration is too low to be detected. Thus, in the last section, we made the conclusion that isolated V_k centers are not necessarily produced in CsI(Na) crystals under ultraviolet irradiation.

REFERENCES

1. C. W. Bates, Jr. Appl Opt. 12 (1973) 938
2. J. Bonanomie and J. Rossel, Helv. Phys. Acta. 25 (1952) 725
3. B. Hahn and J. Rossel, Helv. Phys. Acta. 26 (1953) 803
4. W. Beusch, H. Knoepfel, E. Lopfe, D. Maeder, and P. Stoll, Nuovo Cimento 5 (1975) 575
5. H. Knoepfel, E. Lopfe, and P. Stoll, Helv. Phys. Acta. 29 (1956) 241, and 30 (1957) 521
6. Yu A. Tsirlin, V. I. Startsev and L. M. Soifer, Opt. Spect. 8 (1960) 283
7. A. M. Panova and N. V. Shiran, Bull. Acda. Sci. USSR Phys. Ser. (USA) 35 (1971) 1232
8. T. Sidler, J. P. Pellaux, A. Nouailhat and M. A. Aegerter, Solid State Commun, 13 (1973) 479
9. A. N. Panova and N. V. Shiran, Opt. Spect. (USA) 32 (1972) 108
10. Z. L. Morgenshtern, Opt. Spect. 7 (1959) 146 and 8 (1960) 283
11. P. Brinkmann, Phys. Letters 15 (1965) 305
12. A. N. Panova, K. V. Shakhova and N. V. Shiran, J. Appl. Spect. 6 (1967) 362
13. A. N. Panova and N. V. Shiran, Opt. Spect. (USA) 32 (1972) 55
14. C. W. Bates, Jr., O.L. Hsu, A. Salau, and W. E. Spicer, Phys. Letters 51A (1975) 425
15. C. W. Bates, Jr., I. Schneider, A. Salau and O. L. Hsu, Solid State Commun. 18 (1976) 101
16. O. L. Hsu and C. W. Bates, Jr., J. of Luminesc. 11 (1975) 65
17. O. L. Hsu and C. W. Bates, Jr., "Absorption and Emission due to Localized Excitons in CsI(Na)" (accepted for publication in the Jour. of Luminesc.)
18. O. L. Hsu, Ph.D. thesis, Department of Materials Science and Engineering, Stanford University
19. J. Eby, K. Teegarden and D. B. Dutton, Phys. Rev. 116 (1959) 1099
20. K. Teegarden and G. Baldini, Phys. Rev. 155 (1967) 896
21. H. Lamatsch, J. Rossel and E. Saurer, Phys. Stat. Sol. 41 (1970) 605
22. J. C. Phillips, Phys. Rev. 136 (1964) A1721
23. Y. Onodera, J. Phys. Soc. Japan 25 (1968) 469
24. F. Bassani and N. Inchauspe, Phys. Rev. 105 (1957) 819

25. A. A. Tsertsvadze, Fiz. Tverd. Tela 3 (1961) 336 [Translation: Soviet-Phys.-Sol. State 3 (1961) 241]
26. H. B. Rosenstock, Phys. Rev. 131 (1963) 1111
27. G. A. Rozman, Fiz. Tverd. Tela 7 (1966) 1921 [Translation: Soviet-Phys. - Sol. State 7 (1966) 1555]
28. H. Lamatsch, J. Rossel, and E. Saurer, Phys. Stat. Sol. (b) 46 (1971) 687
29. N. N. Greenwood, Ionic Crystals, Lattice Defects and Non-stoichiometry, Butterworths, London 1968
30. L. Pauling, Proc. Roy. Soc. (London) A114, 181 (1927)
31. J. Pirene and E. Kartheuser, Physica 20 (1964) 2005
32. R. Monnier, Solid State Commun. 19 (1976) 681
33. M. V. Pashkovskii, I.M. Spitkovskii and A. D. Tkachuk, Sov. Phys. - Solid State 11 (1969) 382
34. A. Salau, Ph.D. Thesis, Dept. of Appl. Phys. Stanford Un. (1976)
35. J. J. Pilloud and C. Jaccard, Solid State Commun, 17 (1975) 907
36. H. Lamatsch, J. Rossel and E. Saurer, Phys. Stat. Sol. 41 (1970) 605
37. R. Edgerton, Phys. Rev. 138A (1965) 85
38. N. M. Naumenko and A. N. Panova, Single Crystals, Scintillators and Organic Luminophors" (Kharkov, 1969), No. 5 Part 1, p. 309
39. C. W. Bates, Jr. (Unpublished Results)
40. H. Lamatsch, J. Rossel and E. Saurer, Phys. Stat. Sol. (b) 48 (1971) 311

List of Illustration

- Figure 1. Absorption spectrum of 2mm thick CsI(Na) bulk crystal at 300°K
- Figure 2. Absorption spectrum of 2mm thick CsI(Na) bulk crystal at 195°K
- Figure 3. Absorption spectrum of 2mm thick CsI(Na) bulk crystal at 130°K
- Figure 4. Absorption spectrum of 2mm thick CsI(Na) bulk crystal at 80°K
- Figure 5. Absorption spectrum of 2mm thick CsI(Na) bulk crystal at 40°K
- Figure 6. Absorption spectrum of 2mm thick CsI(Na) bulk crystal at 42°K
- Figure 7. The charge transfer model for an exciton localized in the vicinity of an anionvacancy
- Figure 8. The charge transfer model for an exciton localized in the vicinity of a cation vacancy
- Figure 9. Some of the possible configurations for an exciton created near a defect complex involving a sodium impurity ion
- Figure 10. Several configurations where a sodium "impurity" exciton can be created near a defect-impurity complex
- Figure 11. The difference between the absorption spectra of CsI(Na) before and after UV irradiation at 15°K for 3½ hours.
- Figure 12. Experimental arrangement used to measure emission and excitation spectra
- Figure 13. Characteristic luminescence spectra of CsI(Na) at 300°K and 130°K.
- (a) emission spectrum at 300°K with 245nm excitation
 - (b) excitation spectrum at 300°K for the emission at 425nm
 - (c) emission spectrum at 130°K with 240nm excitation
 - (d) excitation spectrum at 130°K for the emission at 420nm
- Figure 14. Characteristic luminescence spectra of CsI(Na) at 80°K
- (a) Emission spectrum of CsI(Na) at 80°K with 238 nm excitation
 - (b) Excitation spectrum at 80°K for the emission at 410nm
 - (c) Excitation spectrum at 80°K for the emission at 370nm

Figure 15. Characteristic luminescence spectra of CsI(Na) at 40°K

(a) Emission spectrum of CsI(Na) crystal at 40°K with 237nm excitation

(b) Excitation spectrum at 40°K for the emission at 415nm

(c) Excitation spectrum at 40°K for the emission at 370nm

Figure 16. Characteristic Luminescence Spectra of CsI(Na) at 4.2°K

(a) Emission spectrum of CsI(Na) crystal at 4.2°K with excitation at (i) 232nm (ii) 237nm

(b) Excitation spectrum at 4.2°K for the emission at 420nm

(c) Excitation spectrum at 4.2°K for the emission at 380nm

Figure 17. The 345nm emission band of CsI(Na) at various temperatures

(a) at 115°K, excited at 213nm

(b) at 80°K, excited at 213nm

(c) at 40°K, excited at 210nm

(d) at 4.2°K, excited at 210nm

Figure 18. Excitation spectra of the 345nm emission band at

(a) 115°K (b) 80°K (c) 40°K (d) 20°K

Figure 19. The emission spectra of CsI(Na) containing the 310nm emission band

(a) at 130°K, excited at 215nm

(b) at 40°K, excited at 213nm

(c) at 40°K, excited at 217nm

(d) at 20°K, excited at 213nm

Figure 20. The excitation spectra of the 310nm emission in comparison with that of the 345nm emission at (a) 130°K (b) 20°K and (c) 4.2°K

Figure 21. The emission spectra showing the evolution of the 450nm band in terms of excitation energy at (a) 20°K with excitation at (i) 273nm (ii) 257nm (iii) 232nm and (b) 4.2°K with excitation at (i) 273nm (ii) 243nm (iii) 232nm

- Figure 22. The excitation spectrums of the peak and the long wavelength side of the 445nm emission band in comparison with those of the characteristic emission band at (a) 20°K (b) 4.2°K
- Figure 23. The emission spectra of CsI(Na) excited at 219nm at (a) 20°K (b) 4.2°K
- Figure 24. Schematic of the experimental arrangement to determine the relation between the polarization of the excitation and emission light
- Figure 25. Schematic of the experimental arrangement designed to study the involvement of V_k centers in the characteristic luminescent mechanism in CsI(Na) crystal
- Figure 26. The excitation spectra of the 420nm emission band at 77°K from (i) a well-annealed zone-refined CsI(Na) crystal (ii) a CsI(Na) crystal which had been heated to 500°C , kept at that temperature for one hour and cooled to room temperature within four hours
- Figure 27. The emission spectra of CsI(Na) at 4.2°K with excitation at (i) "host" β excitonic band at 228nm (ii) "Impurity" excitonic band at 235nm
- Figure 28. The configuration coordinate diagram which explains the evolution of the two bands of the characteristic emission

List of Tables

- Table 1 The calculated α band wavelengths for the four configurations defined by figure 7 at three temperatures
- Table 2 The calculated wavelengths of excitons localized near a cesium ion vacancy in for configurations defined in Figure 8 at three temperatures.
- Table 3 The calculated energy differences between free and β excitons and β band wavelengths for the four configurations defined by Figure 7 at three temperatures
- Table 4 The calculated wavelengths of "impurity" - exciton bands in the configurations defined in figure 10 at three temperatures

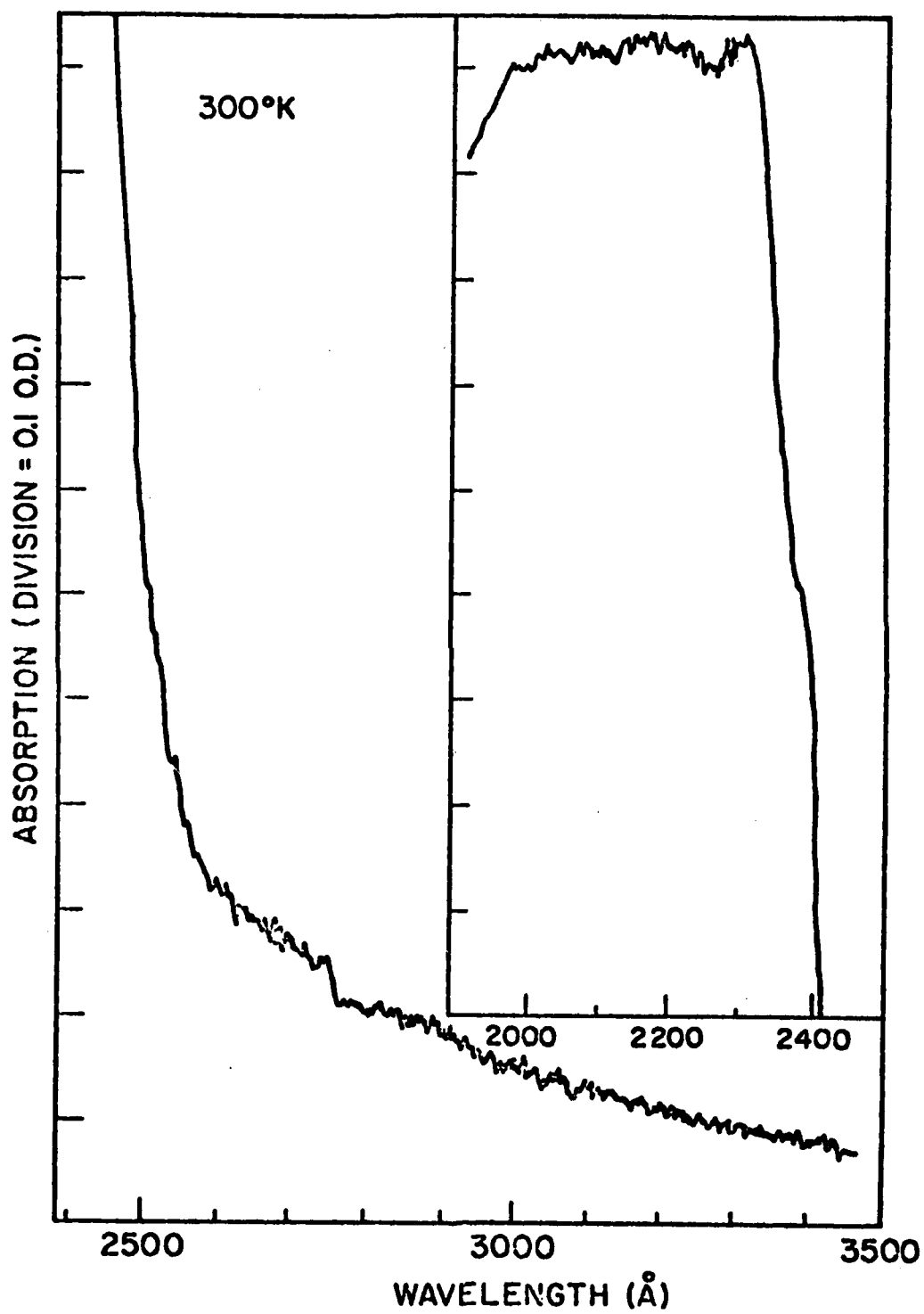


Figure 1. Absorption spectrum of 2mm thick CsI(Na) bulk crystal at 300°K

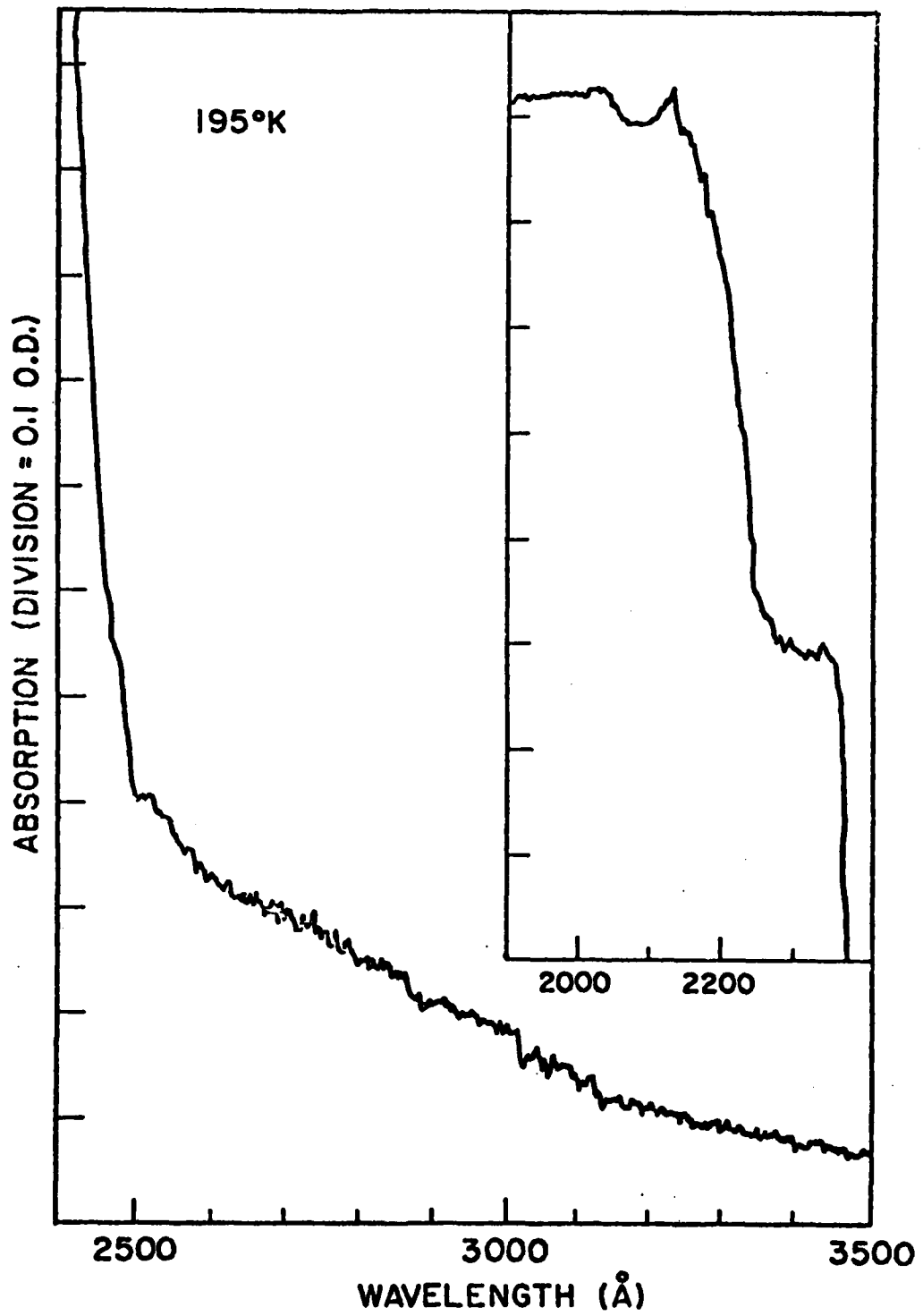


Figure 2. Absorption spectrum of 2mm thick CsI(Na) bulk crystal at 195°K

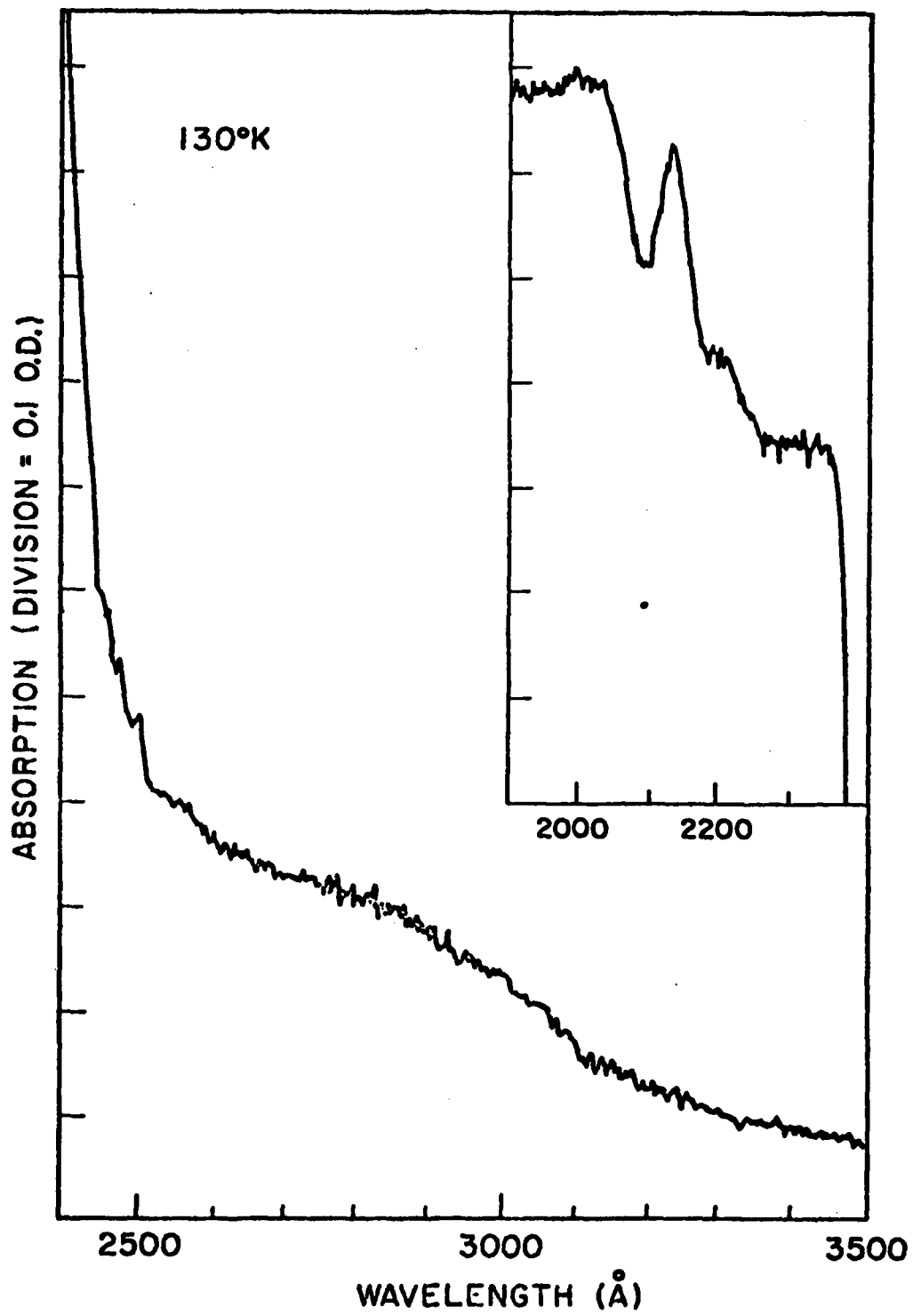


Figure 3. Absorption spectrum of 2mm thick CsI(Na) bulk crystal at 130°K

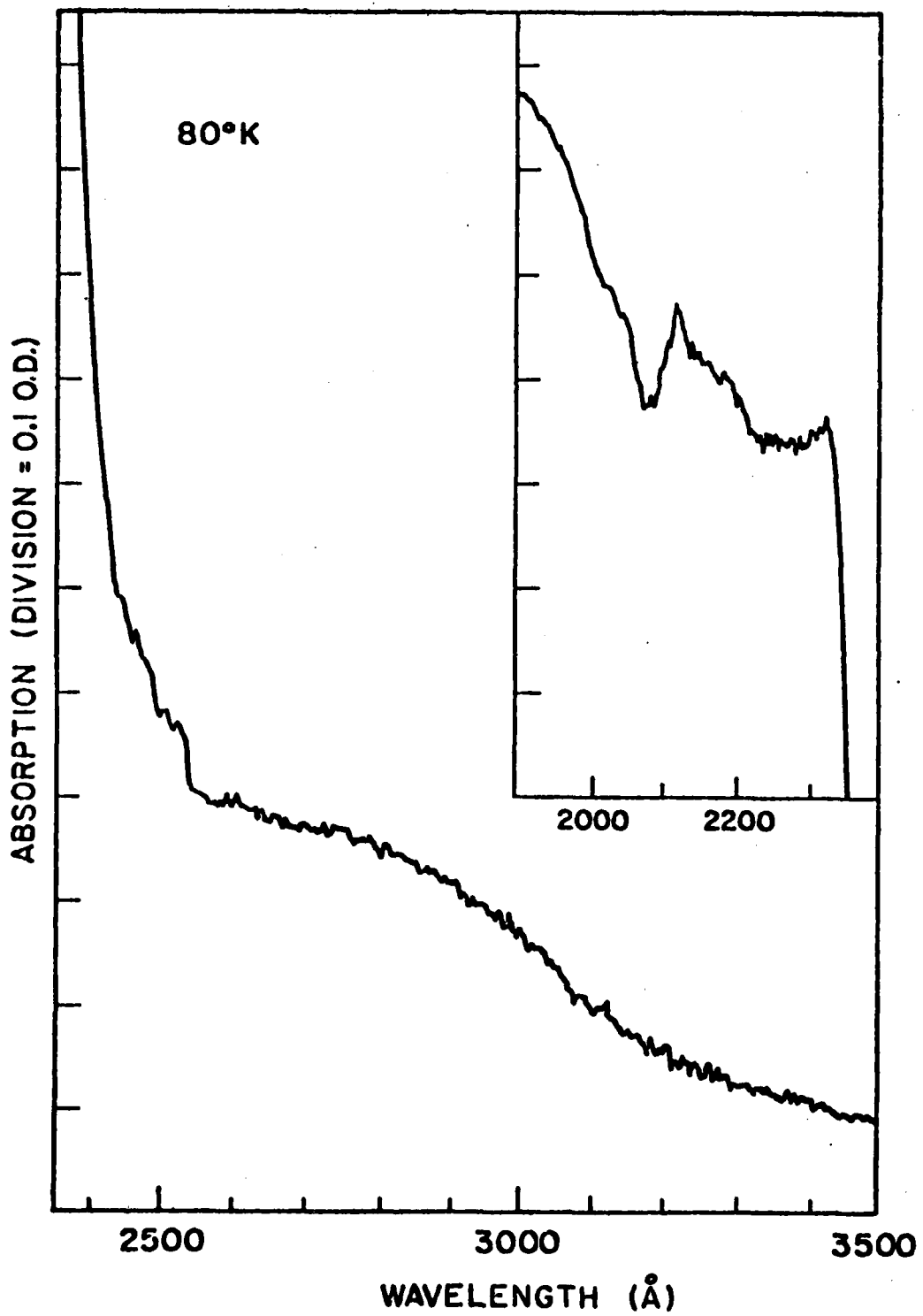


Figure 4. Absorption spectrum of 2mm thick CsI(Na) bulk crystal at 80°K

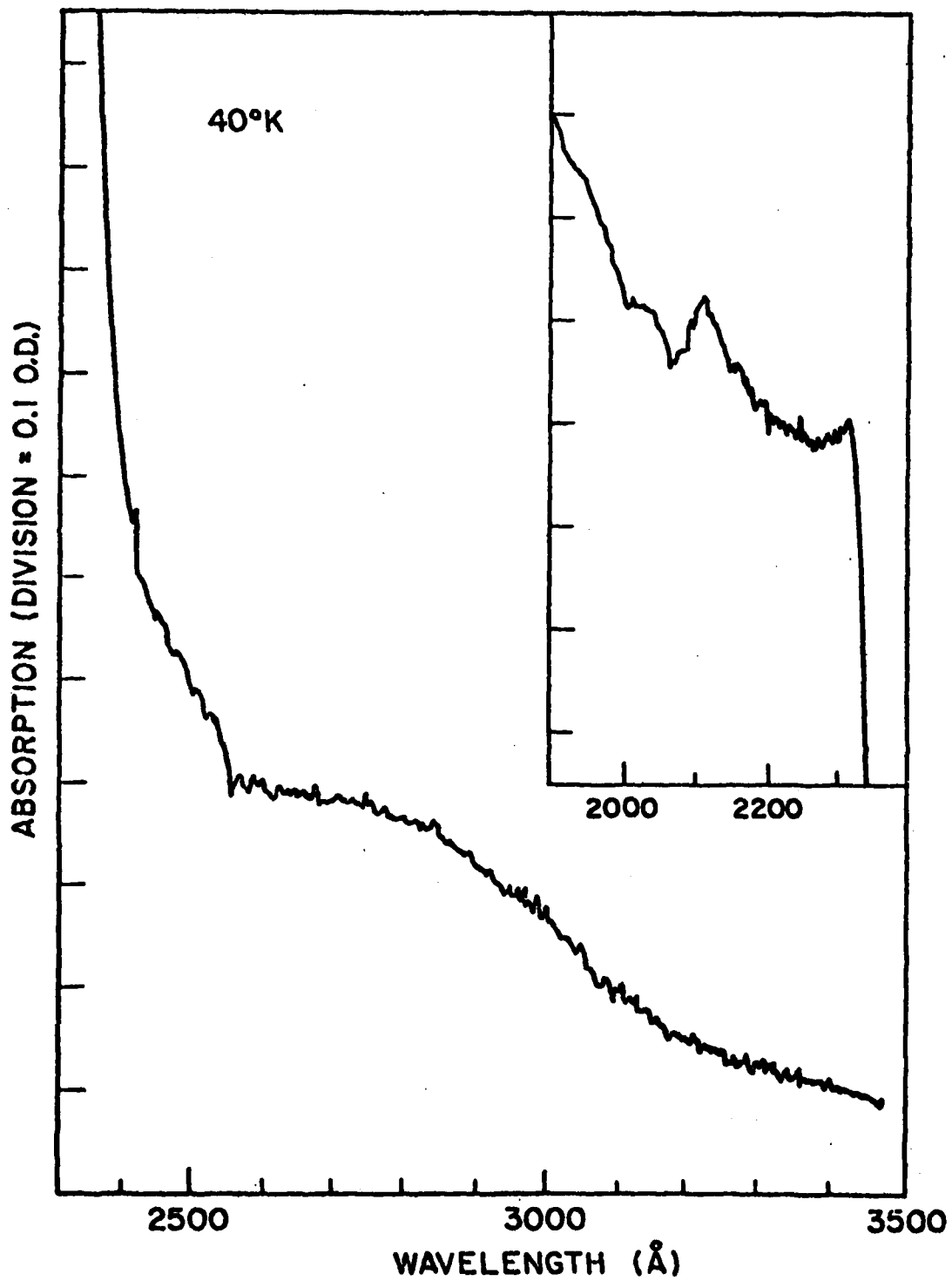


Figure 5. Absorption spectrum of 2mm thick CsI(Na) bulk crystal at 40°K

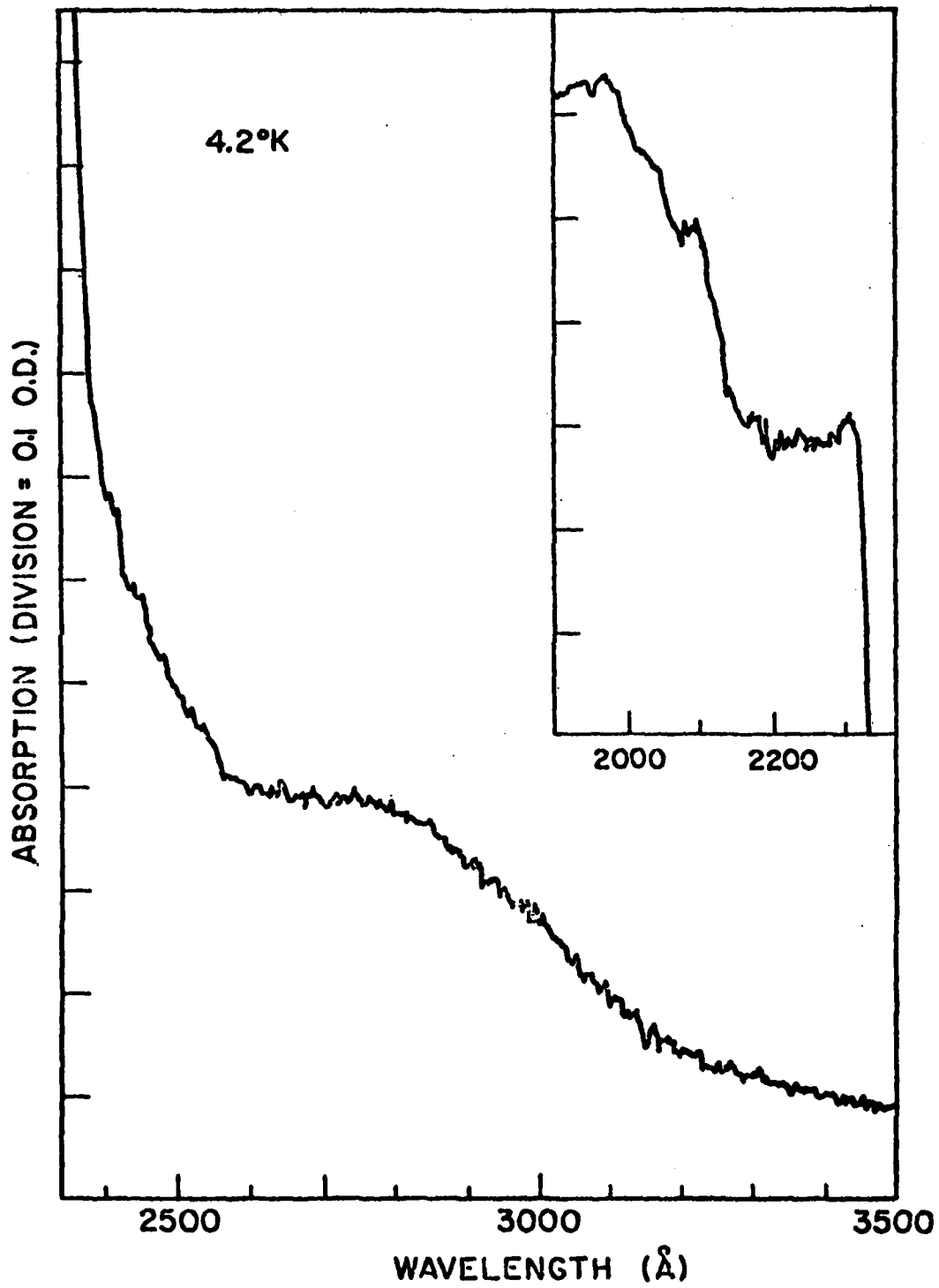


Figure 6. Absorption spectrum of 2mm thick CsI(Na) bulk crystal at 4.2°K

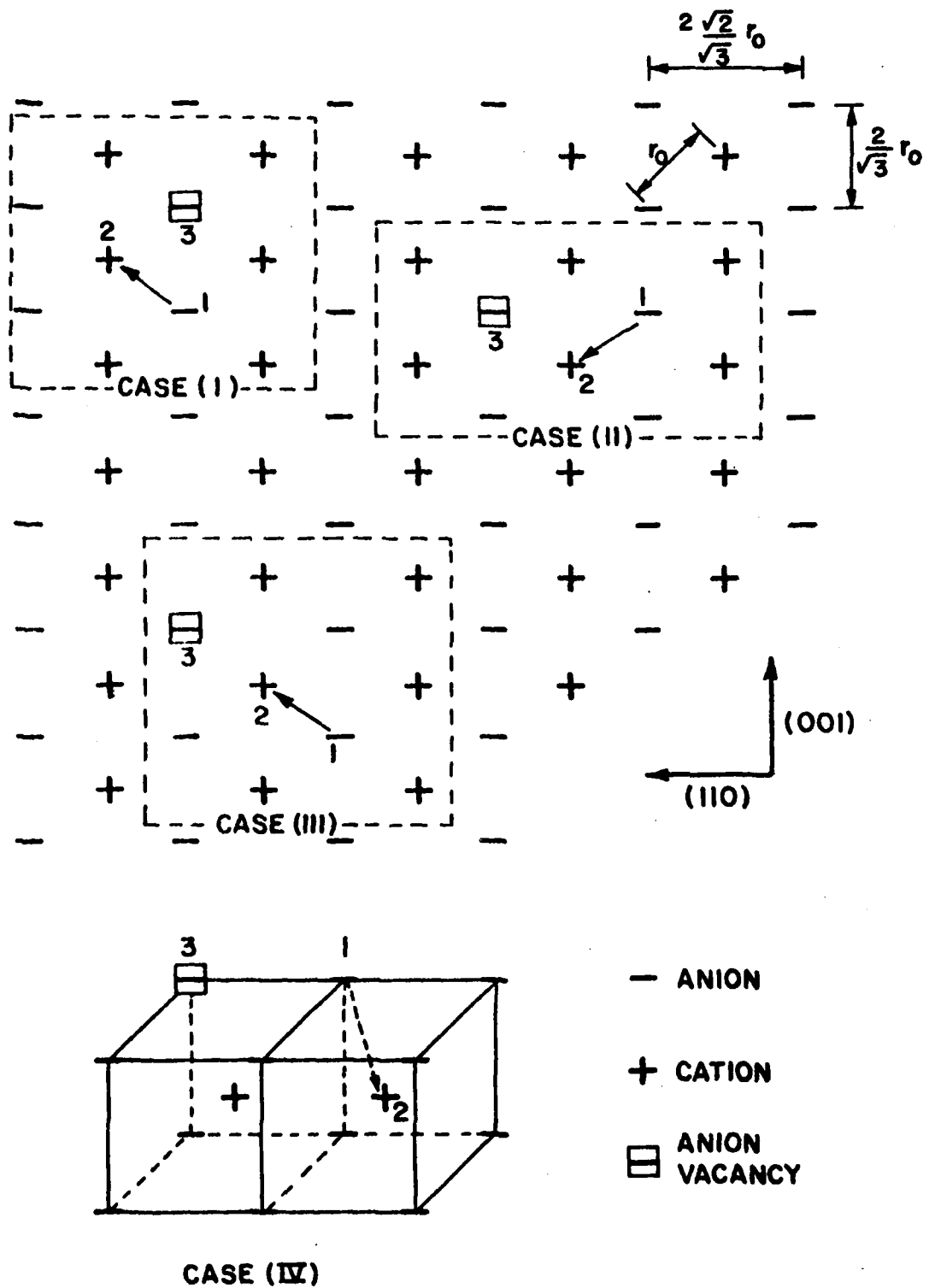


Figure 7. The charge transfer model for an exciton localized in the vicinity of an anion vacancy

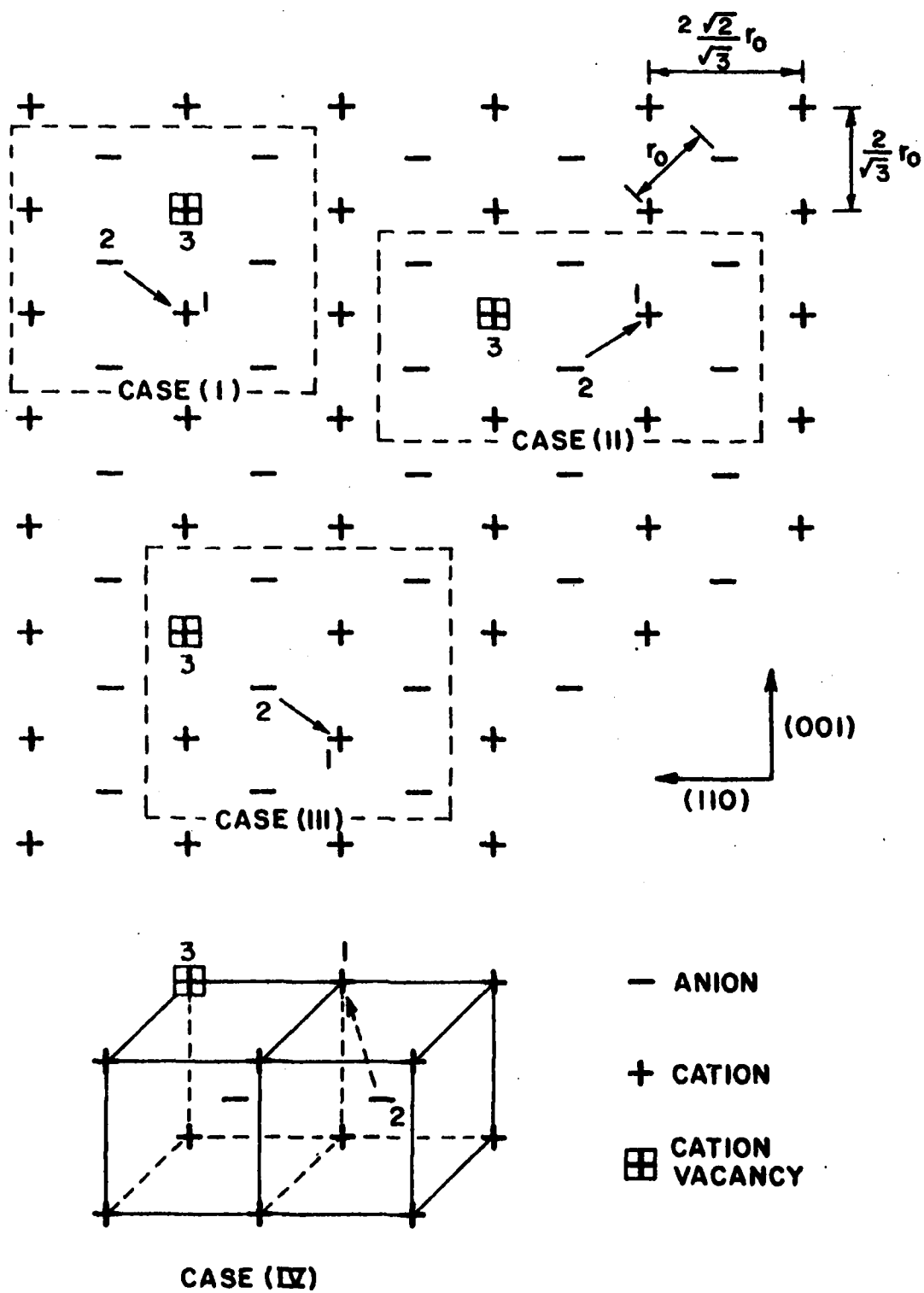
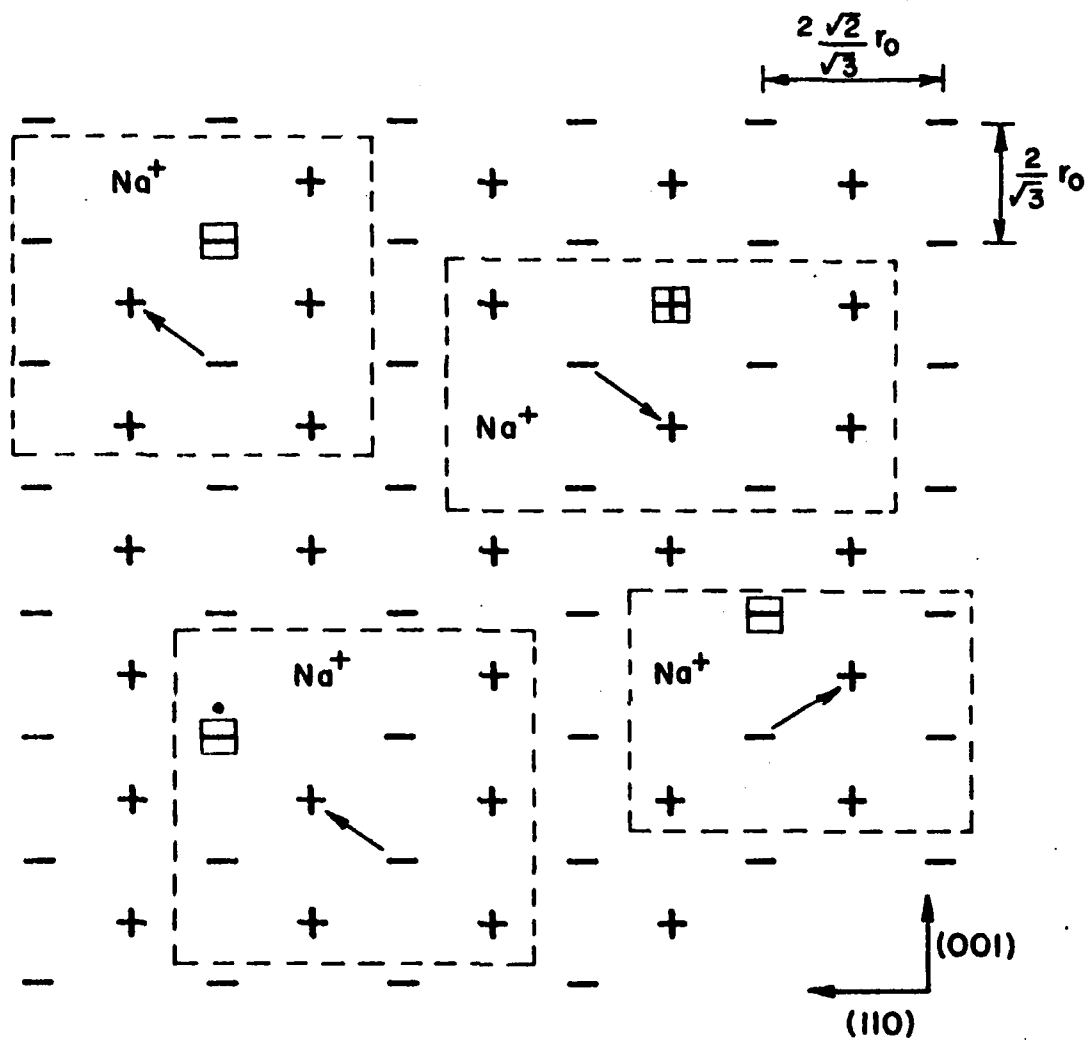


Figure 8. The charge transfer model for an exciton localized in the vicinity of a cation vacancy



- IODINE ION	☐ IODINE ION VACANCY
+ CESIUM ION	⊕ CESIUM ION VACANCY
◻ F CENTER	Na ⁺ SODIUM ION

Figure 9. Some of the possible configurations for an exciton created near a defect complex involving a sodium impurity ion

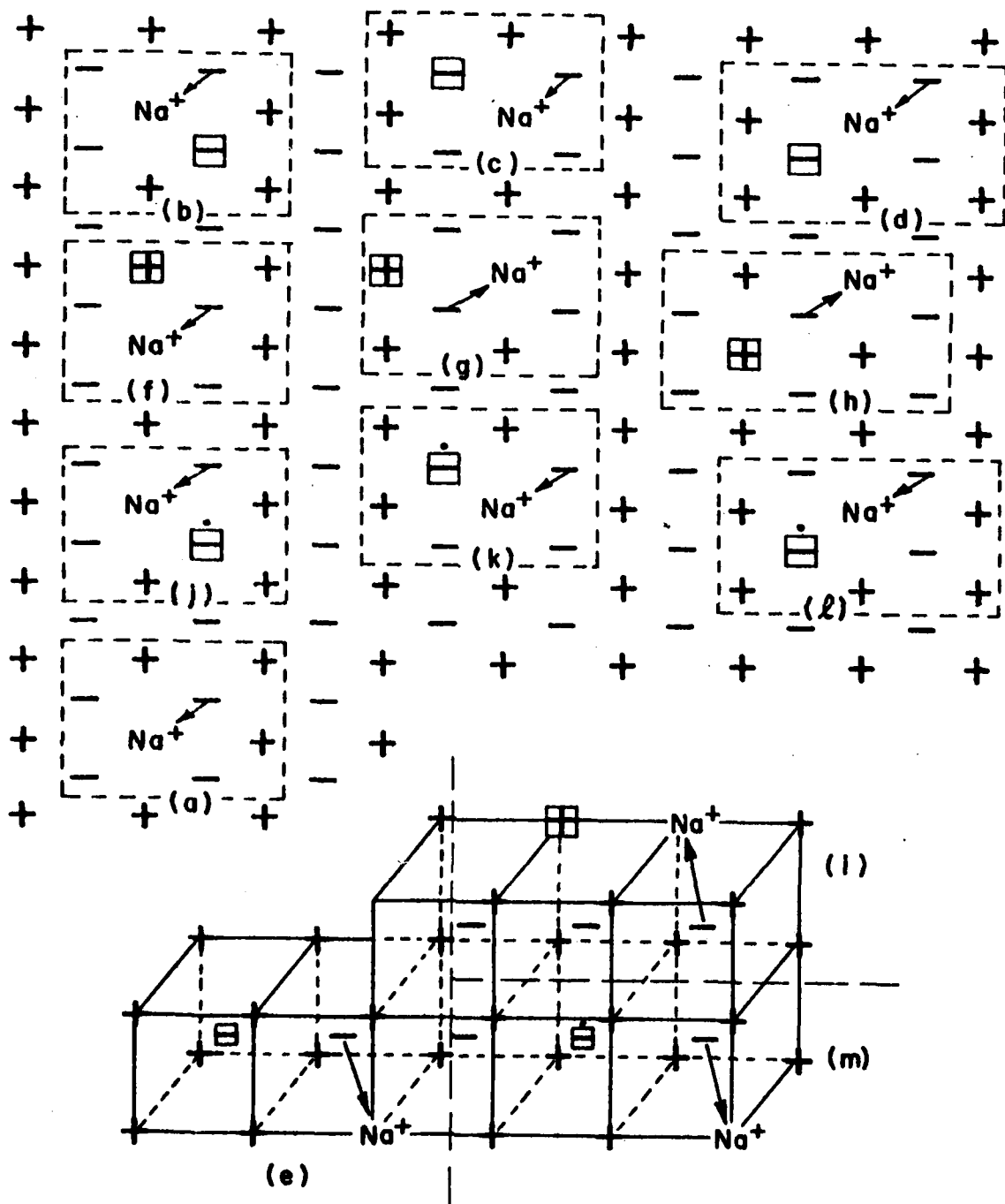


Figure 10. Several configurations where a sodium "impurity" exciton can be created near a defect-impurity complex

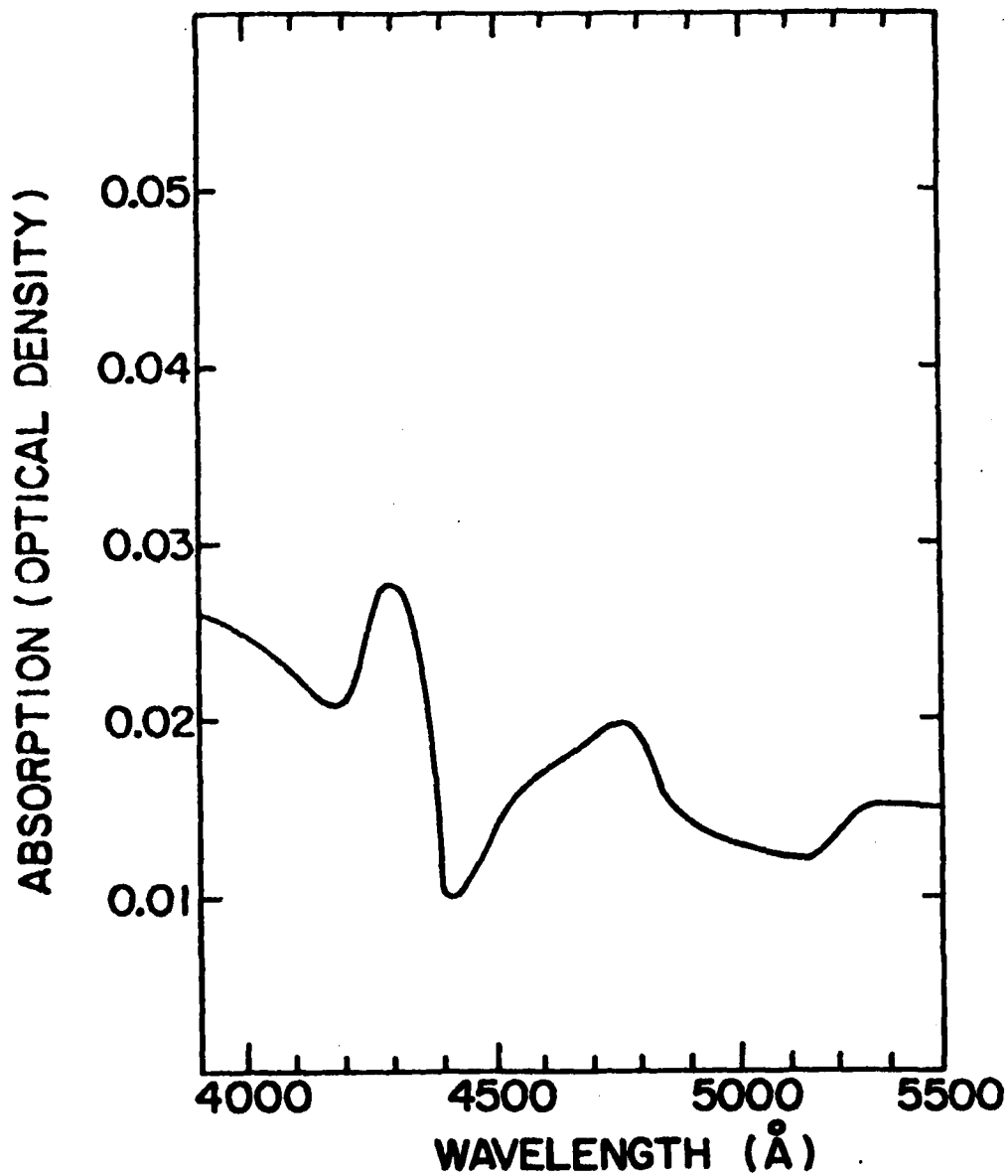


Figure 11. The difference between the absorption spectra of CsI(Na) before and after UV irradiation at 15°K for 3½ hours.

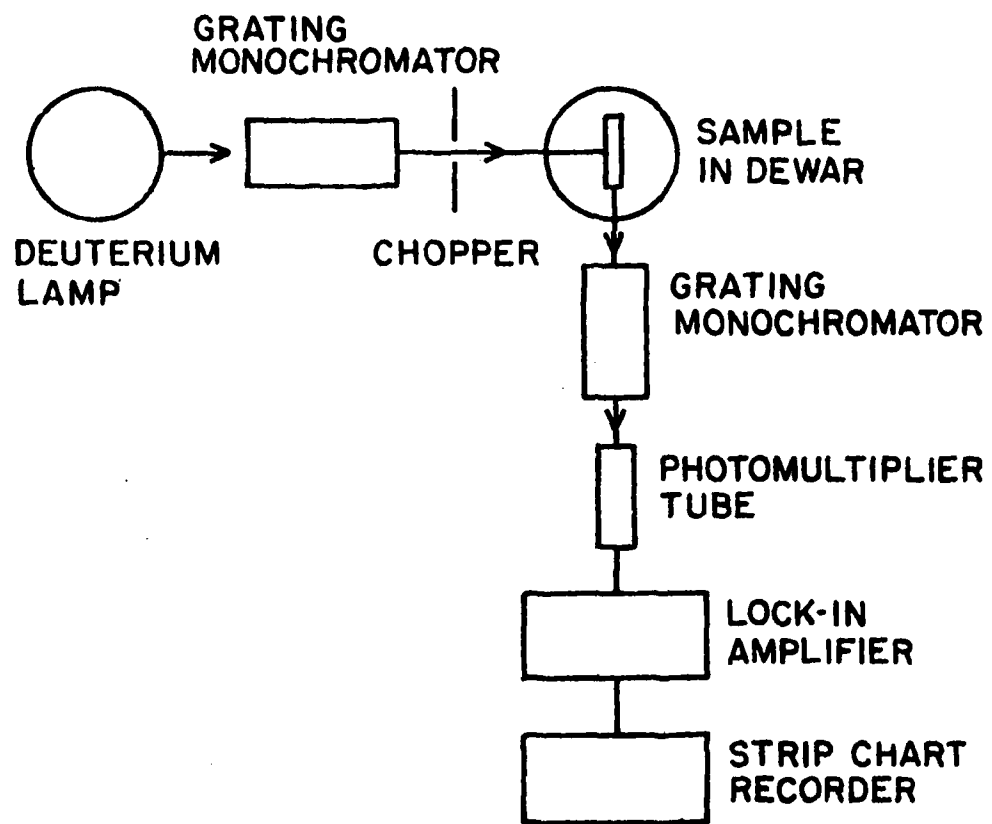


Figure 12. Experimental arrangement used to measure emission and excitation spectra

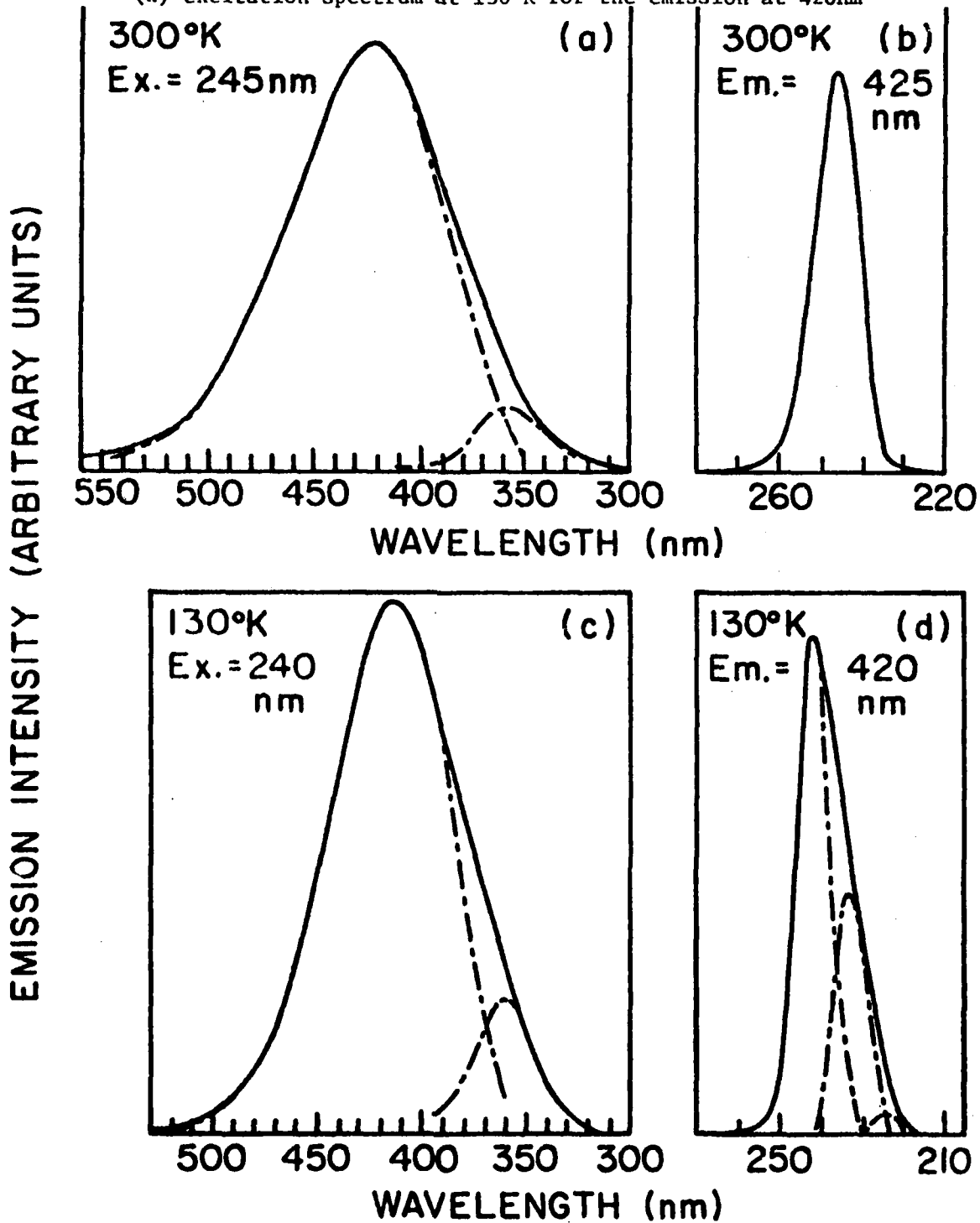
Figure 13. Characteristic luminescence spectra of $\text{CsI}(\text{Na})$ at 300 K and 130 K.

(a) emission spectrum at 300°K with 245nm excitation

(b) excitation spectrum at 300°K for the emission at 425nm

(c) emission spectrum at 130°K with 240nm excitation

(d) excitation spectrum at 130°K for the emission at 420nm



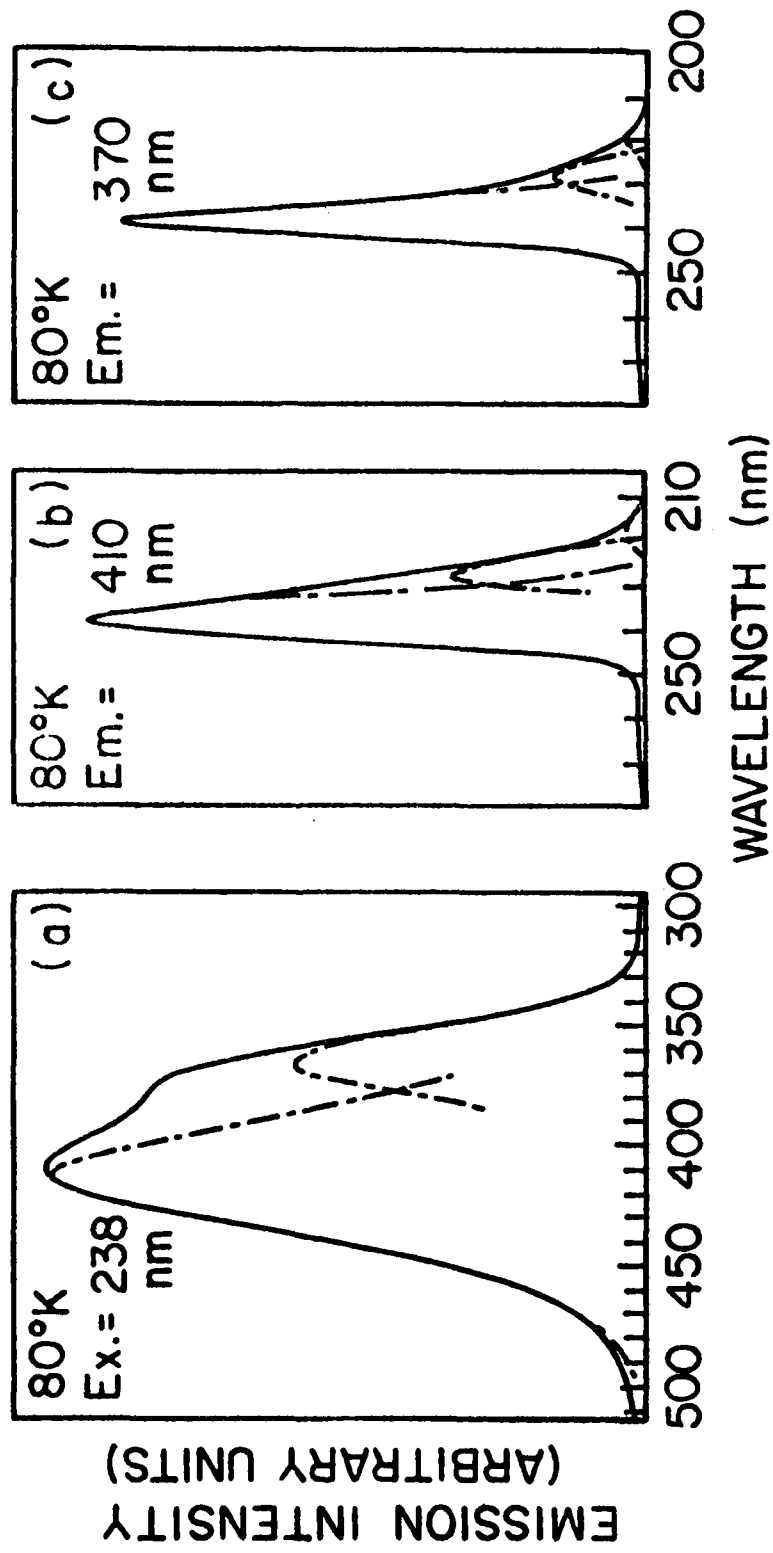


Figure 14. Characteristic luminescence spectra of CsI(Na) at 80°K

(a) Emission spectrum of CsI(Na) at 80°K with 238 nm excitation

(b) Excitation spectrum at 80°K for the emission at 410nm

(c) Excitation spectrum at 80°K for the emission at 370nm

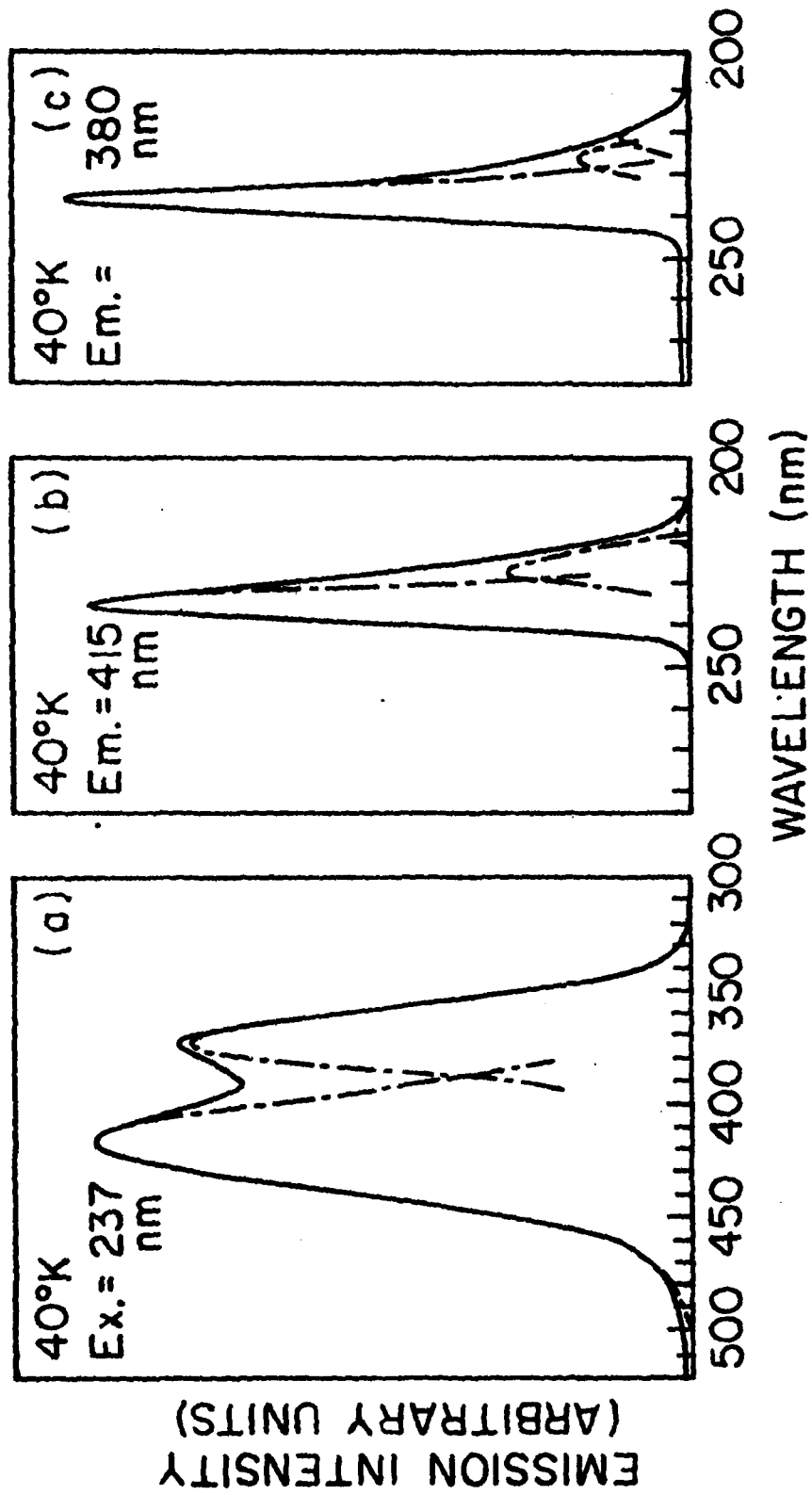


Figure 15. Characteristic luminescence spectra of CsI(Na) at 40°K

(a) Emission spectrum of CsI(Na) crystal at 40°K with 237nm excitation

(b) Excitation spectrum at 40°K for the emission at 415nm

(c) Excitation spectrum at 40°K for the emission at 380nm

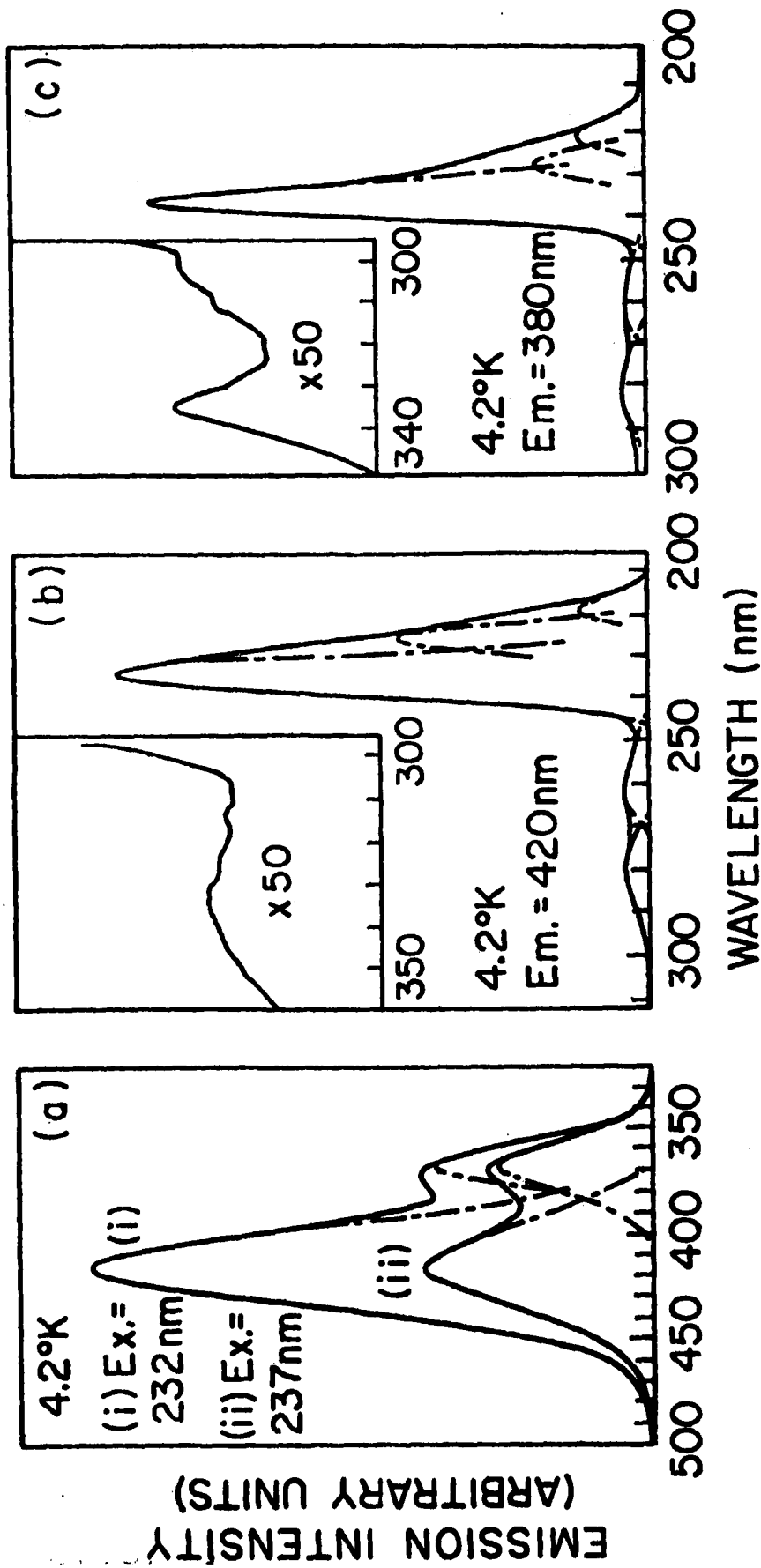


Figure 16. Characteristic Luminescence Spectra of CsI(Na) at 4.2°K
 (a) Emission spectrum of CsI(Na) crystal at 4.2°K with excitation at (i) 232nm (ii) 237nm
 (b) Excitation spectrum at 4.2°K for the emission at 420nm

EMISSION INTENSITY (ARBITRARY UNITS)

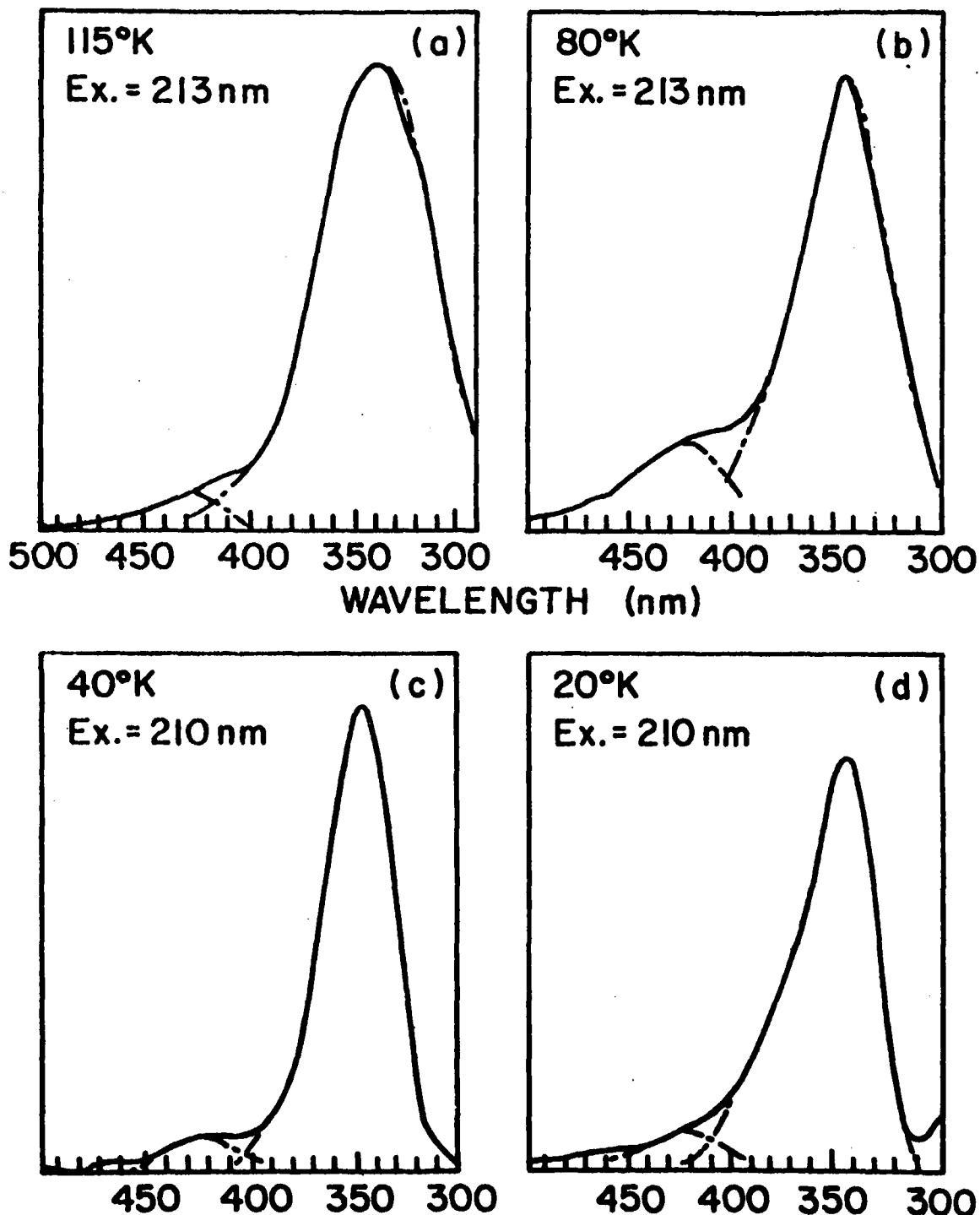


Figure 17. The 345nm emission band of CsI(Na) at various temperatures

(a) at 115°K, excited at 213nm

(b) at 80°K, excited at 213nm

(c) at 40°K, excited at 210nm

(d) at 4.2°K, excited at 210nm

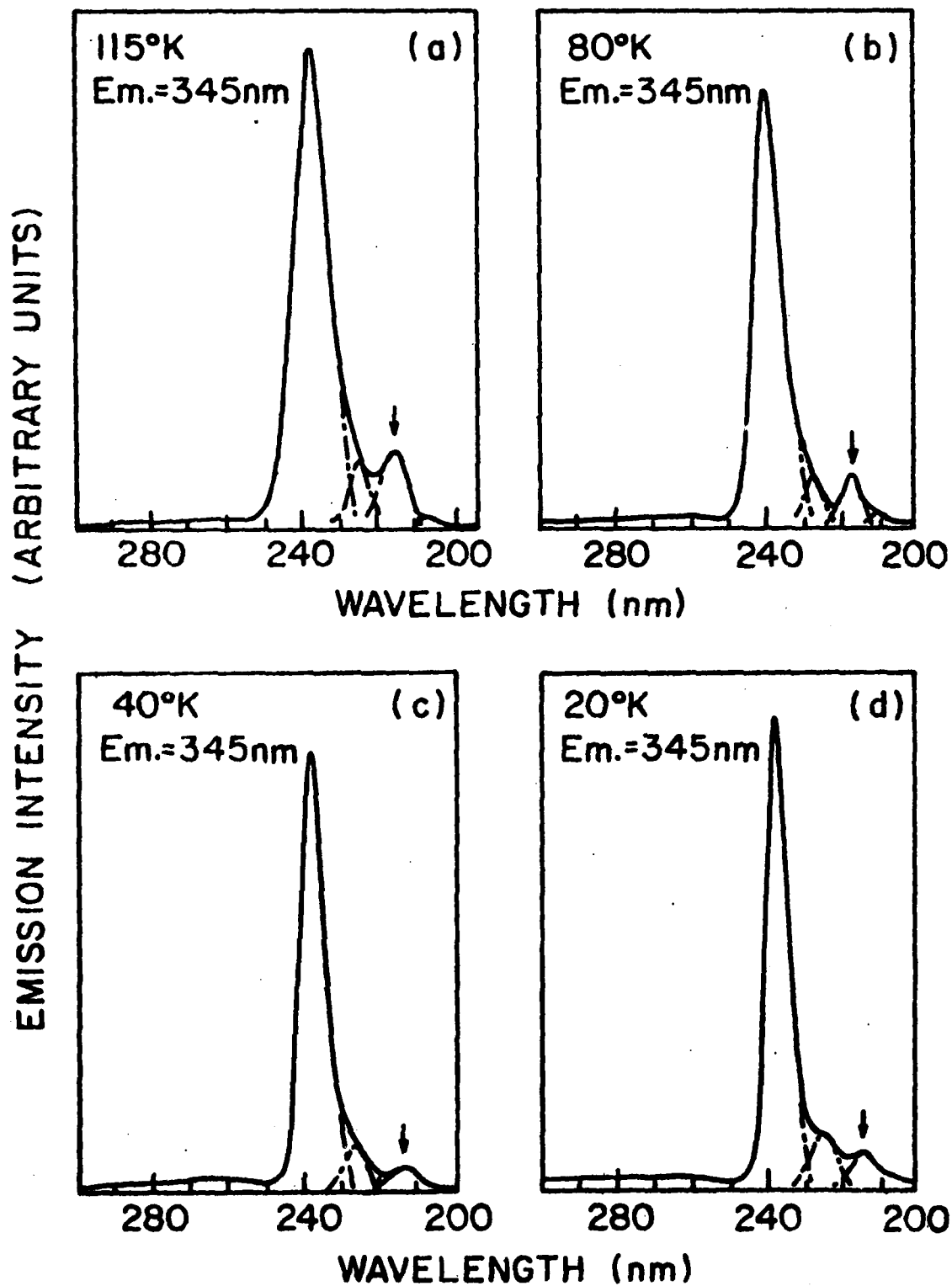


Figure 18. Excitation spectra of the 345nm emission band at:
 (a) 115°K (b) 80°K (c) 40°K (d) 20°K

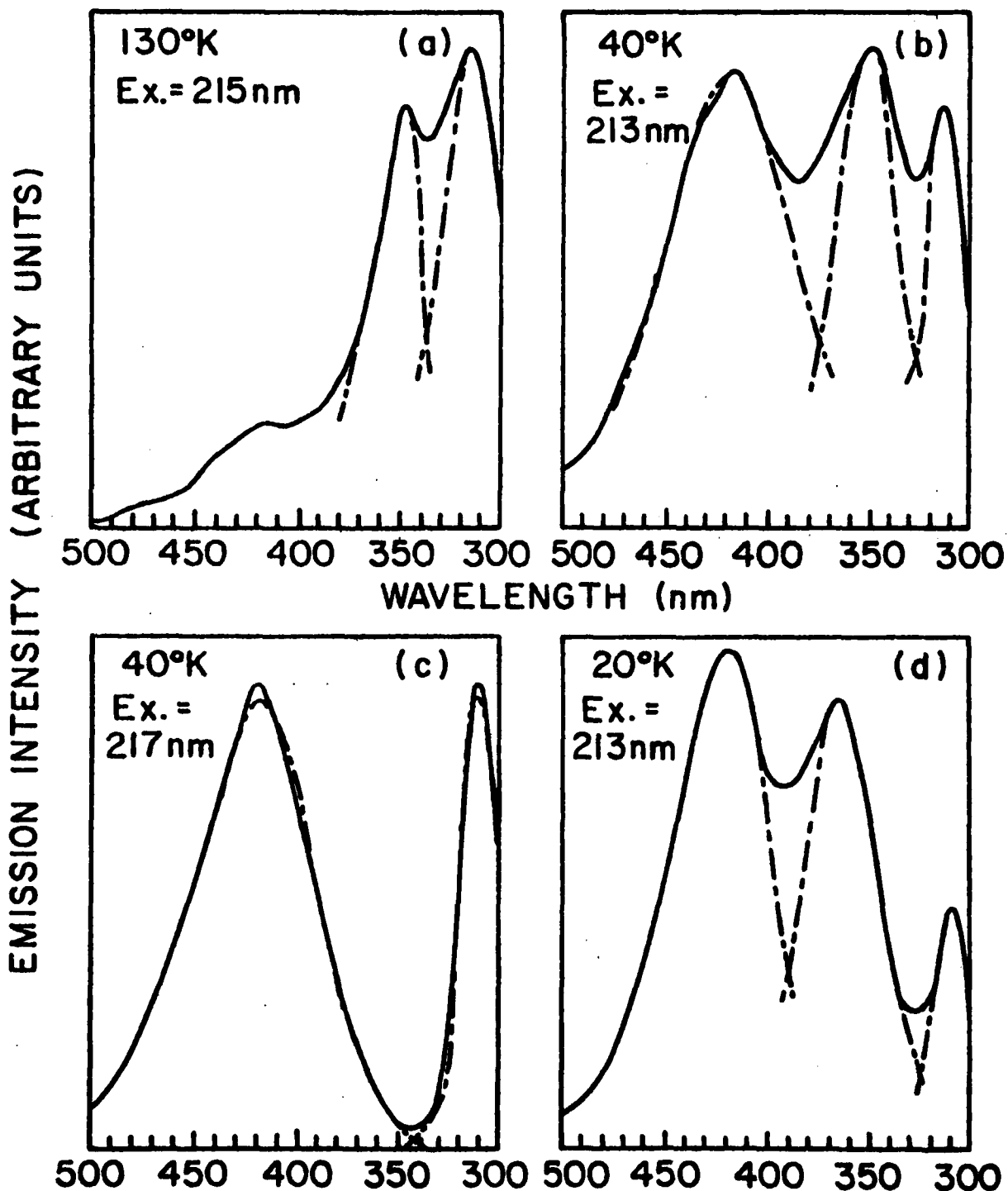


Figure 19. The emission spectra of CsI(Na) containing the 310nm emission band

(a) at 130°K, excited at 215nm

(b) at 40°K, excited at 213nm

(c) at 40°K, excited at 217nm

(d) at 20° K, excited at 213nm

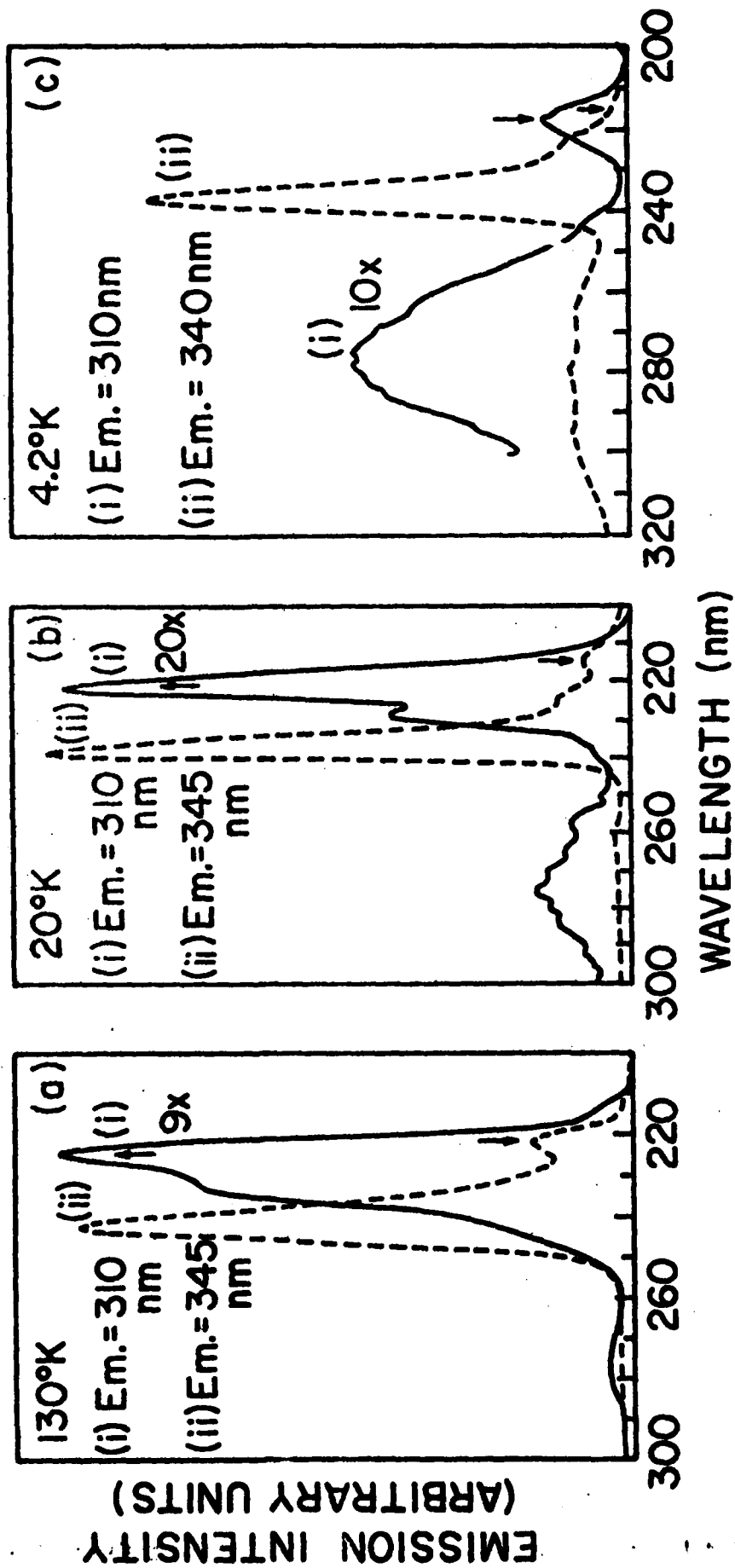


Figure 20. The excitation spectra of the 310nm emission in comparison with that of the 345nm emission at (a) 130°K (b) 20°K and (c) 4.2°K

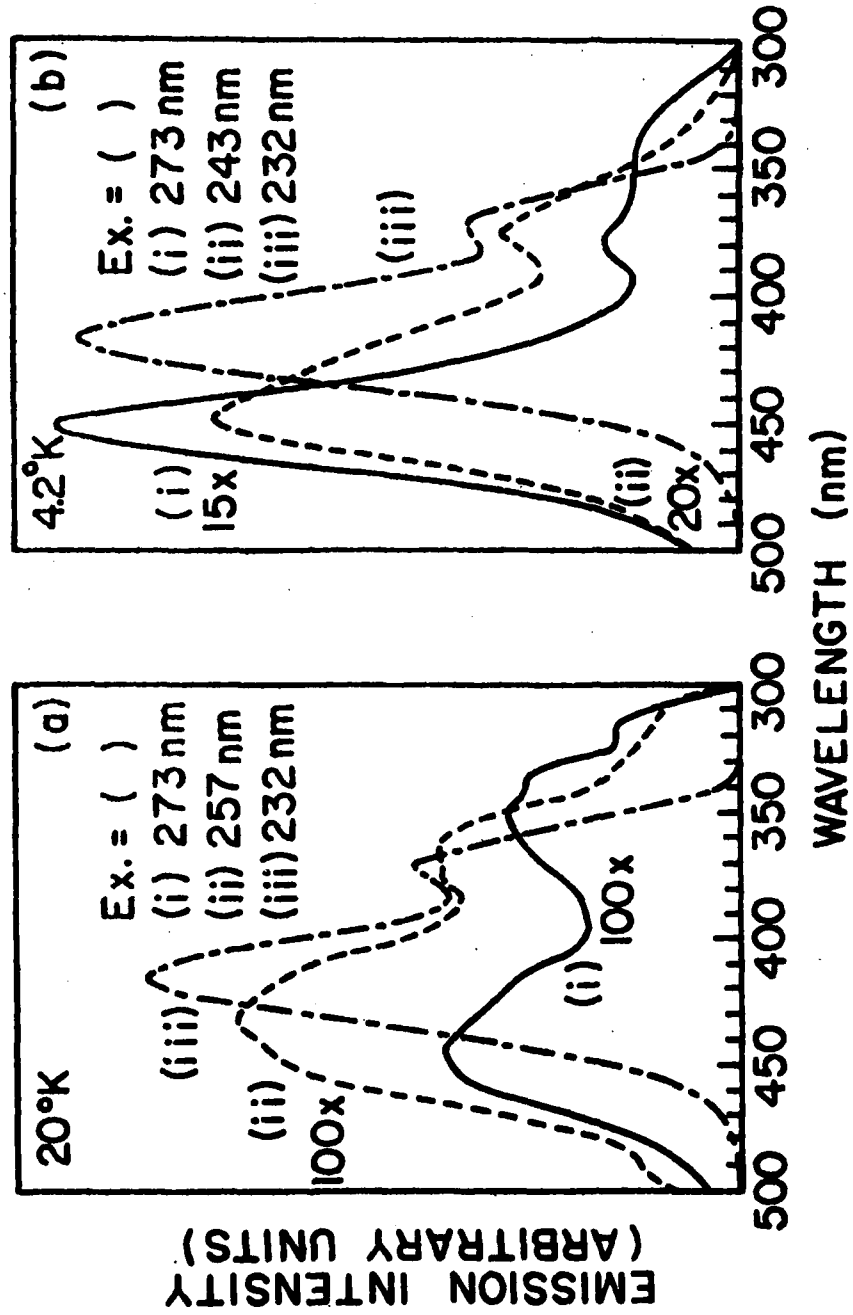


Figure 21. The emission spectra showing the evolution of the 450nm band in terms of excitation energy at (a) 20°K with excitation at (i) 273nm (ii) 257nm (iii) 232nm and (b) 4.2°K with excitation at (i) 273nm (ii) 243nm (iii) 232nm

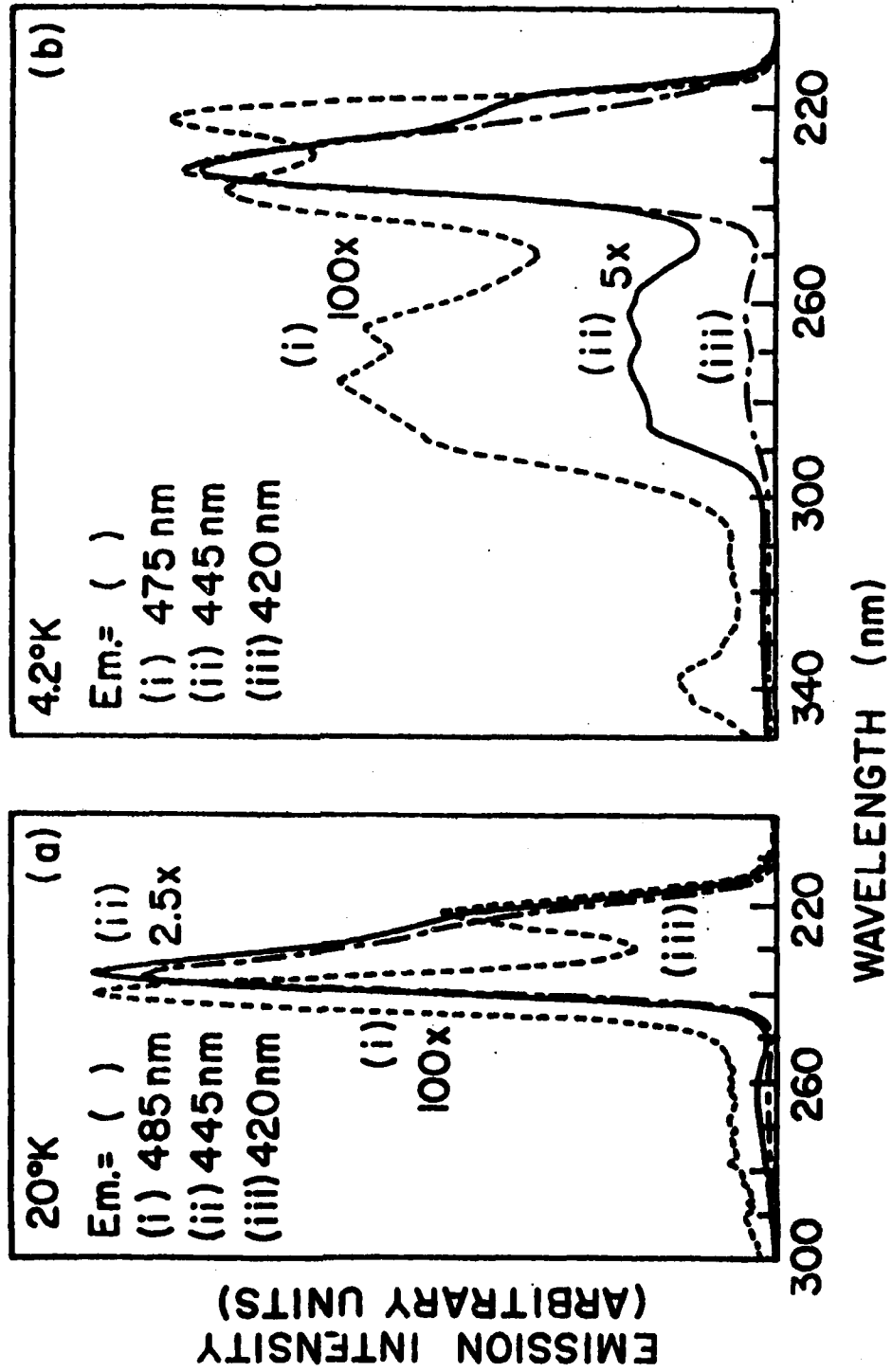


Figure 22. The excitation spectra of the peak and the long wavelength side of the 445nm emission band in comparison with those of the characteristic emission band at (a) 20°K (b) 4.2°K

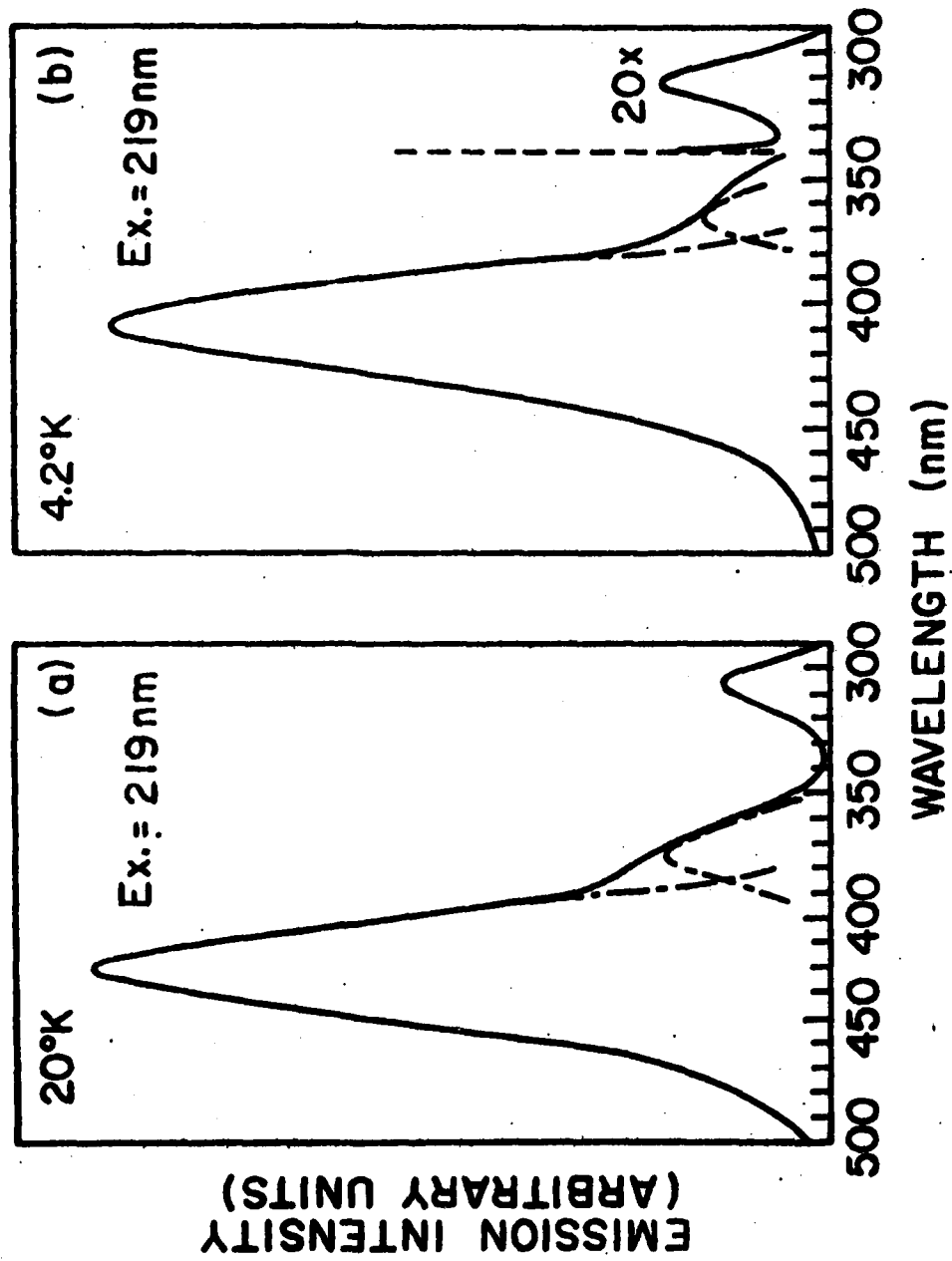


Figure 23. The emission spectra of CsI(Na) excited at 219nm at (a) 20°K

(b) 4.2°K

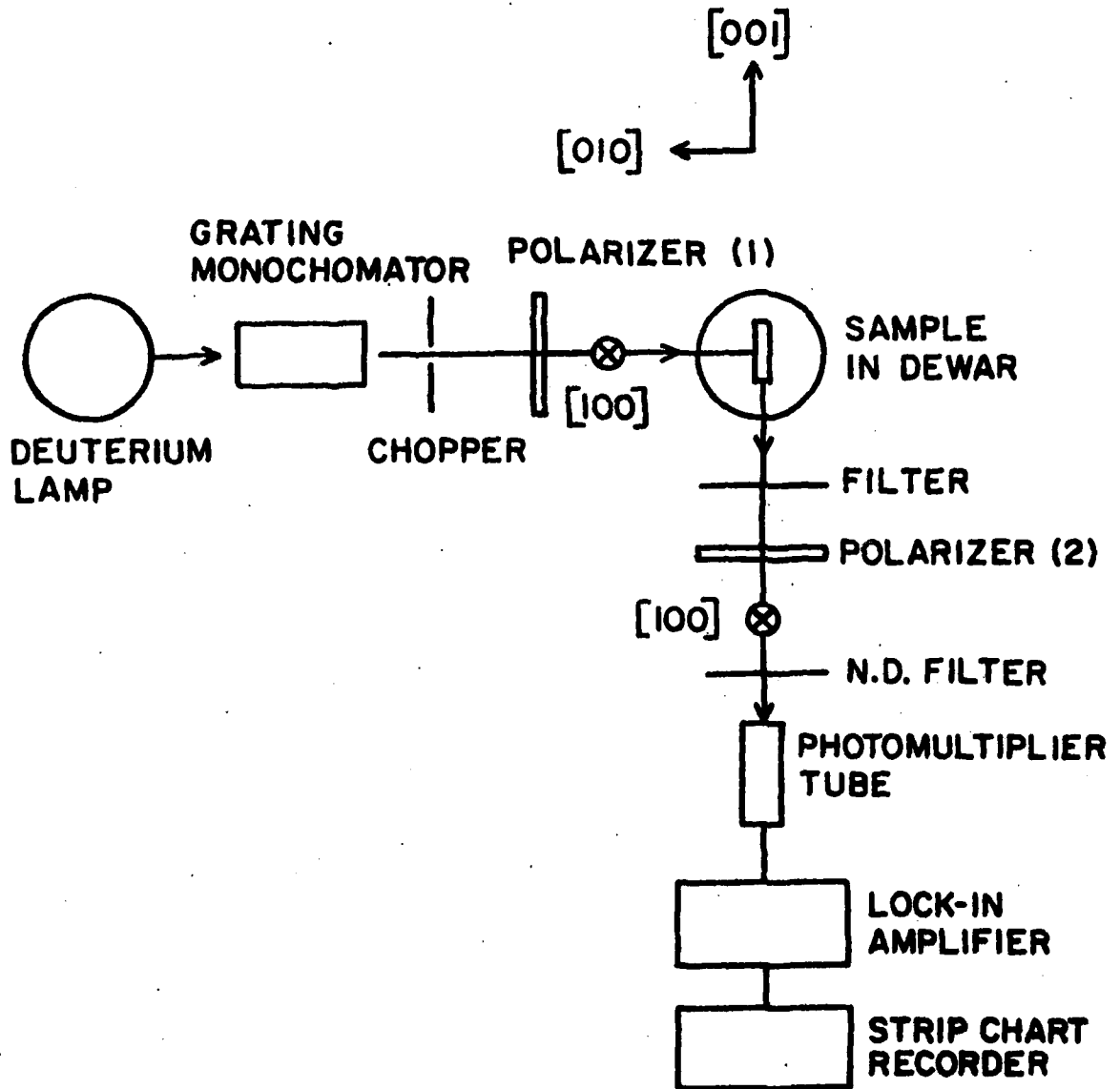


Figure 24. Schematic of the experimental arrangement to determine the relation between the polarization of the excitation and emission light

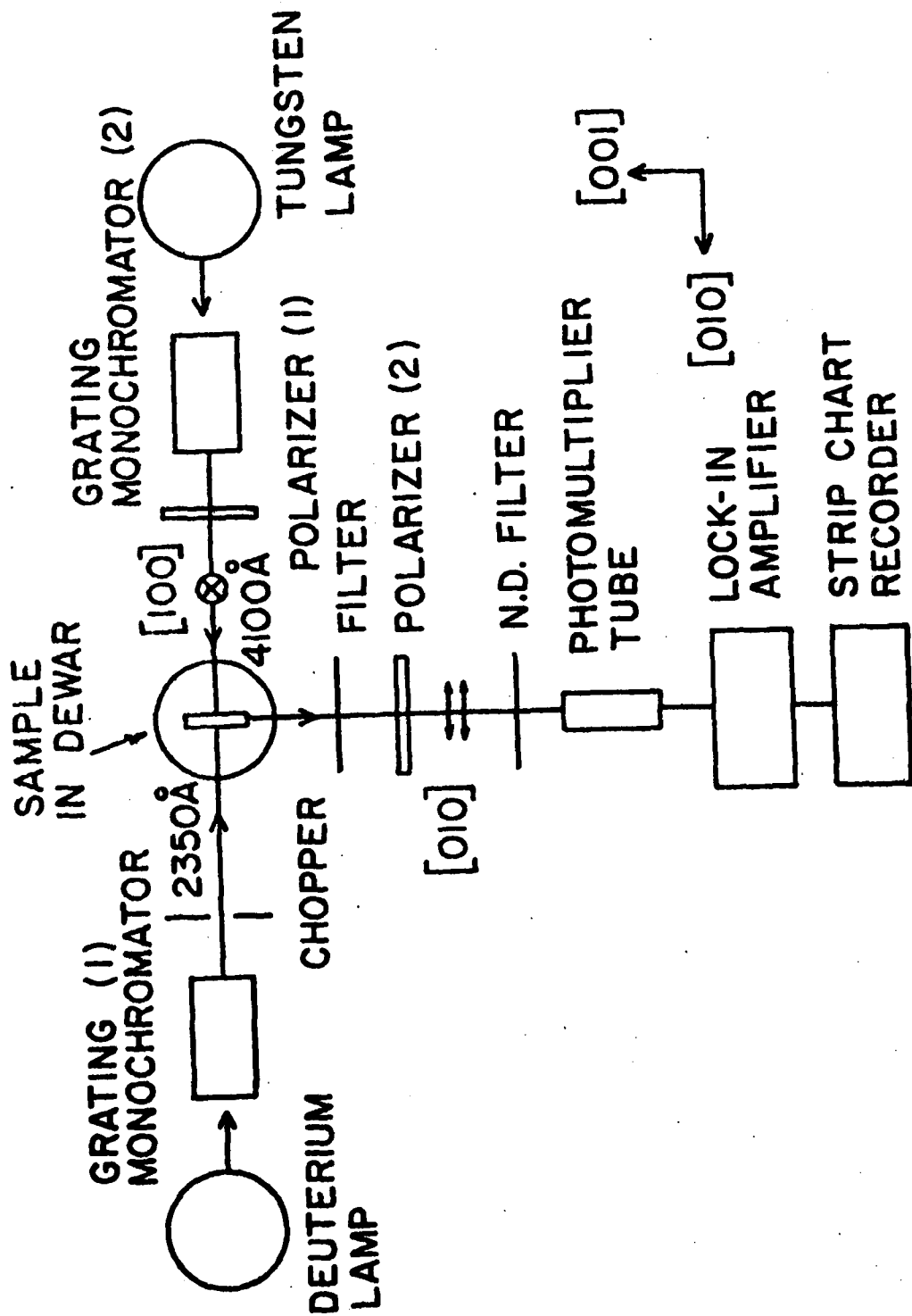


Figure 25. Schematic of the experimental arrangement designed to study the involvement of V_k centers in the characteristic luminescent mechanism in CsI(Na) crystal

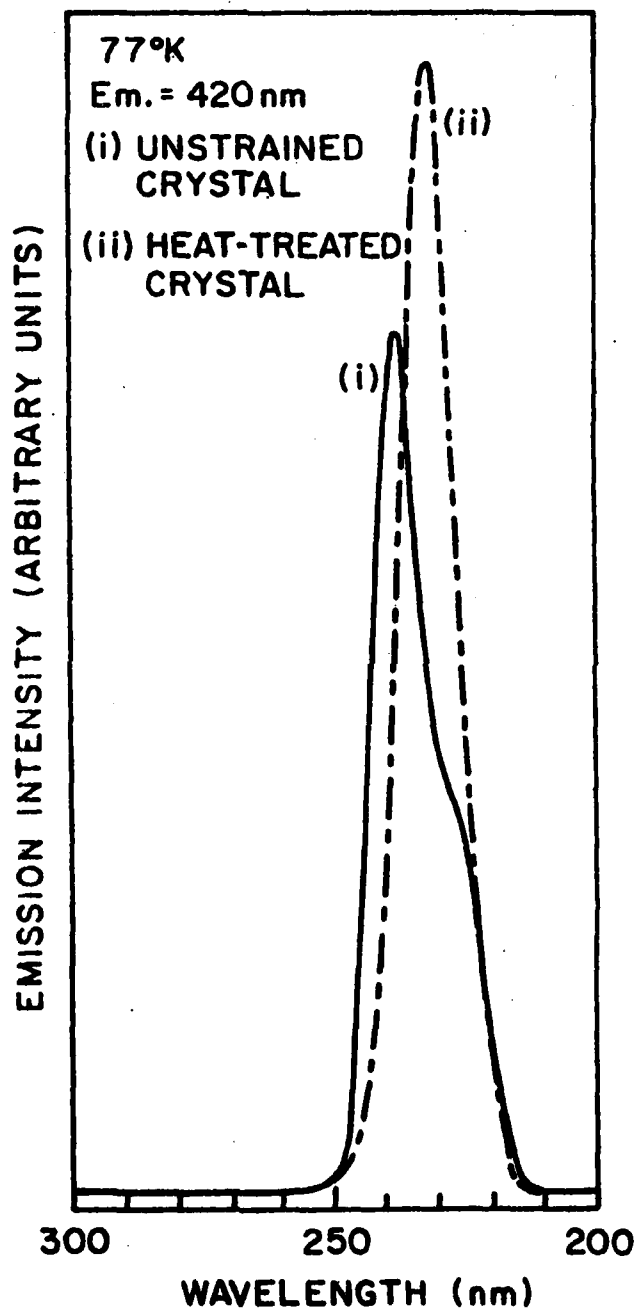


Figure 26. The excitation spectra of the 420nm emission band at 77°K from (i) a well-annealed zone-refined CsI(Na) crystal (ii) a CsI(Na) crystal which had been heated to 500°C, kept at that temperature for one hour and cooled to room temperature within four hours

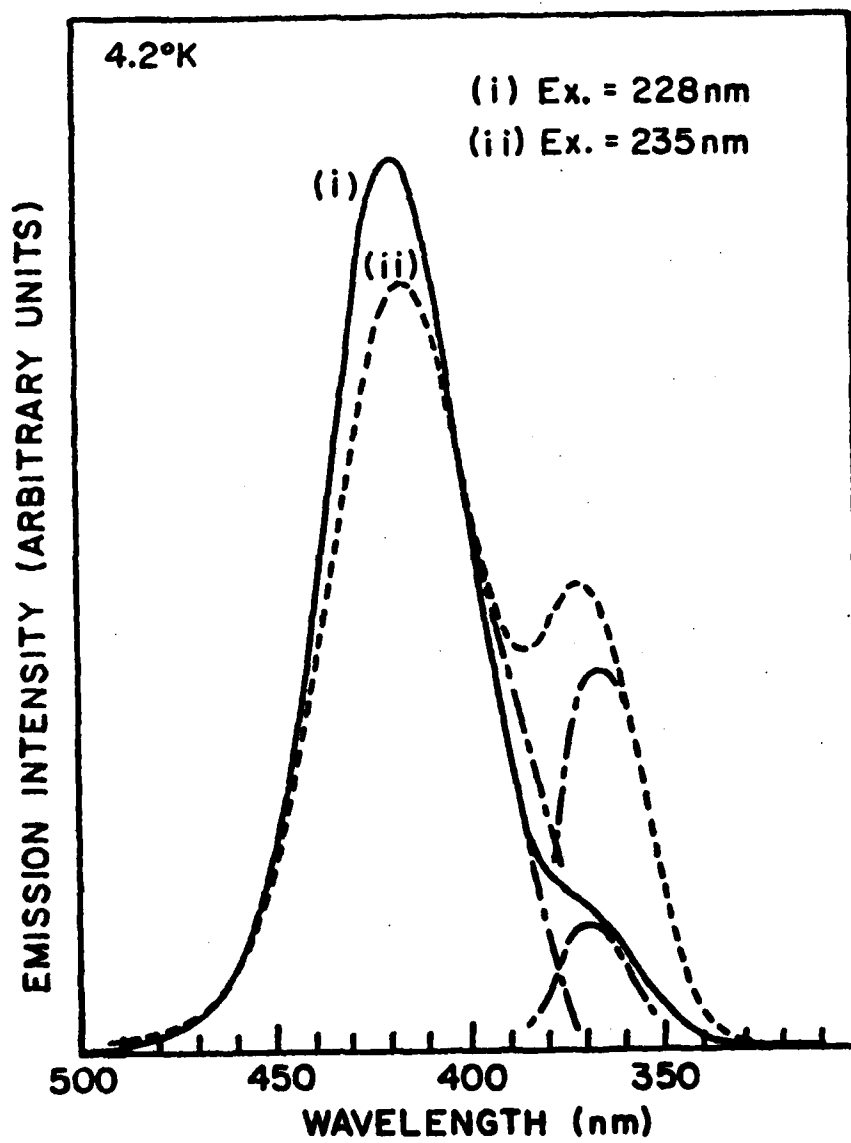


Figure 27. The emission spectra of CsI(Na) at 4.2°K with excitation at (i) "host" β excitonic band at 228nm (ii) "Impurity" excitonic band at 235nm

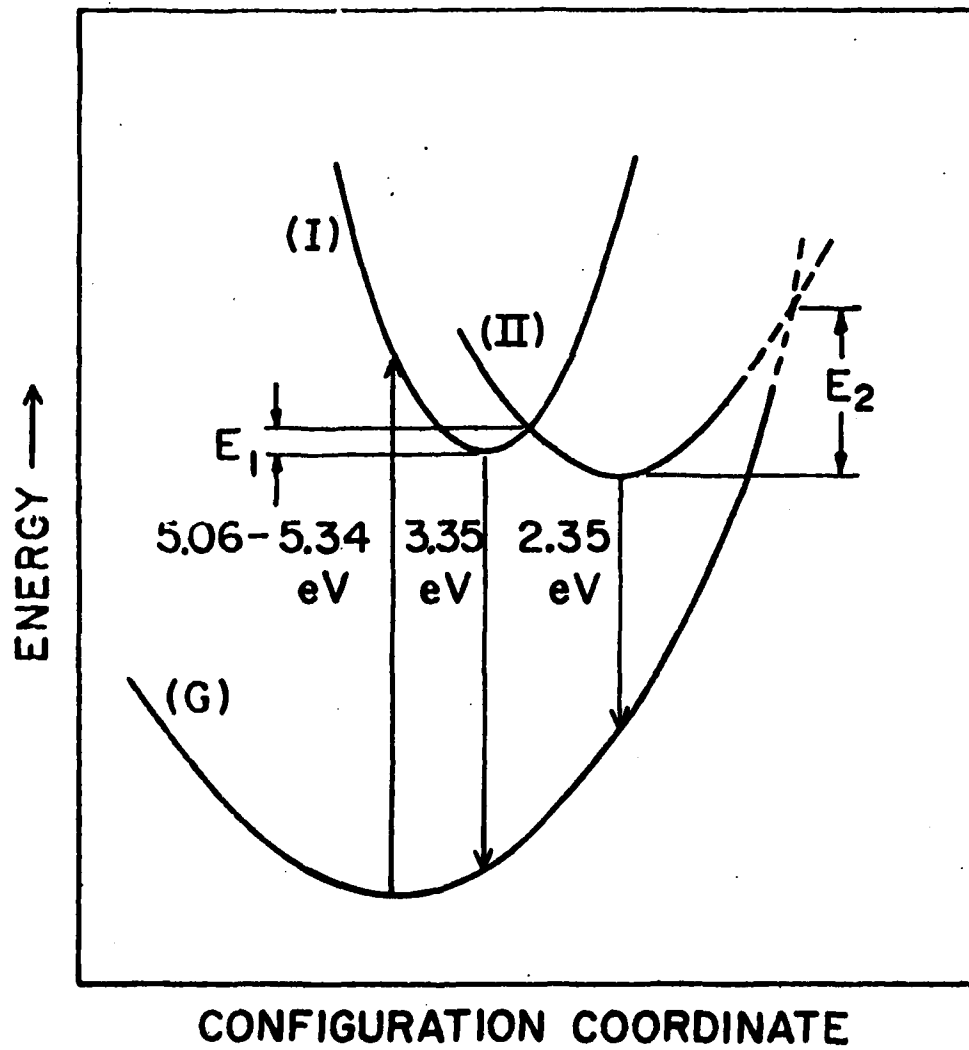


Figure 28. The configuration coordinate diagram which explains the evolution of the two bands of the characteristic emission

Table 1: The calculated α band wavelength for the four configurations defined in figure 7 at three temperatures

		Case (I)	Case (II)	Case (III)	Case (IV)
$h\nu_f - h\nu_l$		0.003	0.109	0.137	0.106
λ_α (Å)	300°K	2230	2270	2280	2270
	77°K	2155	2195	2205	2190
	4.2°K	2135	2175	2185	2175

Table 2: The calculated wavelengths of excitons localized near a cesium ion vacancy in four configurations defined in figure 8 at three temperatures.

		Case (I)	Case (II)	Case (III)	Case (IV)
$h\nu_f - h\nu_{Cs\ vac.}$		0.092	0.117	0.203	0.172
$\lambda_{Cs\ vac.}$ (Å)	300°K	2260	2270	2310	2300
	77°K	2190	2200	2230	2220
	4.2°K	2170	2180	2210	2200

Table 3: The calculated energy differences between free and β excitons and β band wavelengths for the four configurations defined by figure 7 at three temperatures.

		Case (I)	Case (II)	Case (III)	Case (IV)
$h\nu_f - h\nu_\beta$	300°K	0.451	0.327	0.352	0.198
	77°K	0.426	0.308	0.332	0.188
	4.2°K	0.383	0.275	0.297	0.172
λ_β	300°K	2420	2365	2380	2310
	77°K	2325	2275	2285	2225
	4.2°K	2285	2240	2250	2200

TABLE 4
 The Calculated Wavelengths of "impurity"-Exciton Bands
 in the Configurations Defined in Fig. 10
 at Three Temperatures

Case	300°K	77°K	4.2°K	
(a)	2420	2335	2315	"impurity" exciton
(b)	2425	2335	2315	"impurity" exciton localized near an iodine ion vacancy ("impurity" α exciton)
(c)	2475	2385	2360	
(d)	2490	2400	2370	
(e)	2475	2385	2360	
(f)	2465	2375	2355	"impurity" exciton localized near a cesium ion vacancy
(g)	2480	2390	2365	
(h)	2520	2430	2405	
(i)	2505	2415	2390	
(j)	2655	2540	2490	"impurity" exciton localized near an F center ("impurity" β exciton)
(k)	2590	2480	2440	
(l)	2600	2490	2450	
(m)	2520	2420	2390	

DATE
FILME
- 8